Discover Applied Sciences

Research

Risk exposure in recycled agro-industrial waste: radioactive sources and potential effects

Solomon Oyebisi[1]

Received: 6 January 2025 / Accepted: 3 April 2025
Published online: 12 April 2025

Abstract
There is a growing interest in evaluating radionuclides of recycled waste materials due to the potential health risks associated with naturally occurring radioactive materials. This study investigated and evaluated the risk exposure in recycled agro-industrial wastes, often disposed of in landfills or lagoons but are increasingly used as building and construction materials. Datasets were sourced from relevant peer-reviewed articles. The activity concentrations (^{226}Ra, ^{232}Th, and ^{40}K) of recycled agro-industrial waste were assessed, and other radioactive risk parameters were evaluated based on these values. The radiological parameters were analyzed using multivariate item techniques to identify similarities and correlations between the radioactive parameters. The results revealed that all agricultural byproducts met the permissible world average limits. However, all industrial byproducts exceeded these limits except for marble powder, pyrite ash, silica fume, steel slag, and waste glass powder. The Pearson correlation coefficients and factor analysis showed that the ^{40}K isotope significantly influences the radionuclide activities of agricultural byproducts, accounting for 71.20% of the variability. The ^{232}Th concentration significantly contributes to the radionuclide activities of industrial byproducts, with variability ranging from 50.20 to 58.20%. These findings provide a robust radiological safety framework for using agro-industrial byproducts and propose new techniques for reducing the radiological risks of industrial byproducts. The study also underscores the importance of assessing the radiation risks associated with the potential use of agro-industrial byproducts.

Article Highlights

- Surveyed agricultural byproducts pose no radioactive risk.
- Most industrial byproducts studied pose radioactive risks.
- Agricultural and industrial byproducts are significantly influenced by ^{40}K and ^{232}Th.

Keywords Agricultural waste materials · Industrial waste materials · Radiation protection · Radioactive waste · Waste management

✉ Solomon Oyebisi, sotech281.ola@gmail.com | [1]Civil Engineering and Geomatics Department, Durban University of Technology, Durban, South Africa.

1 Introduction

The demand for raw materials has increased due to the global population. By 2050, it is anticipated that the worldwide cement and concrete market will have doubled, raising carbon emissions and endangering biodiversity [1]. Cement production is responsible for approximately 6 and 8% of the greenhouse gas and carbon dioxide (CO_2) emissions. These contexts call for prompt strategies to reduce the adverse impacts of cement production on climate change [1]. One of the scientific and technological means of achieving material sustainability is to recycle agro-industrial wastes of natural origins and compositions to produce building materials [2]. The available study reported that out of 9,176.68 million metric tons of industrial waste generated in 2011, only 64.45% was collected [3].

Agro-industrial wastes are wastes generated from agricultural and industrial activities. Recycling is an innovative circular economy technology that enhances resource sustainability by using waste and reducing primary resource utilization [4]. Recycling agro-industrial wastes as supplementary cementitious materials (SCMs) offers environmental, economic, and product benefits. This concept has gained increasing attention and has become an emerging practice in replacing cement replacement. It mitigates the adverse environmental problems intrinsic to the energy consumption and CO_2 emissions associated with cement production. The agro-industrial byproducts are used as SCMs in concrete production [5].

The built environment faces challenges driving its activities toward sustainable development due to materials' poor management and recycling technologies [6]. Natural radioactivity is present in industrial wastes, byproducts, and agricultural wastes (pozzolans) [7]. Recycling agro-industrial wastes as building materials emits alpha, beta, and gamma radiation [7]. Notwithstanding the technical, economic, and environmental advantages of recycled agro-industrial waste materials [8], their impact on human health is essential to guarantee the safety of integrated materials [9]. Using agro-industrial byproducts as supplementary cementitious materials (SCMs) in blended cement production causes a dose contribution to building inhabitants due to bulk concrete being inbuilt [9]. Previous studies reported that recycled industrial wastes contain heavy or undesirable chemicals that adversely condition their utilization as SCMs [2]. As a result, an in-depth evaluation of such SCMs is required before their use as building materials. Most building materials are derived from various locations and have geological and geographical properties. An assessment of the radioactive content levels in those materials is required to determine human radiation exposure [10]. Radiation protections were introduced by various standard organizations to regulate the concentration limits of building materials and issue restrictions on materials with excessive natural radionuclides [7, 11–13]. Radioactivity is a common irradiation source by which naturally occurring or artificial nuclides pass through spontaneous decay and release new energy. Radioactivity is measured in Becquerel (Bq). Becquerel is the quantified activity of radioactive material through which one nucleus decays per second [14].

Humans are naturally exposed to natural radionuclides [15]. These radionuclides are formed and released into water and air by different meteorological agents, such as oxidation and reduction. In the air, the main element is ^{222}Rn, which, as it decays over time, results in ^{210}Pb. In the soil, the main element is ^{40}K; in the water, the main element is ^{238}U series, while ^{232}Th and their descendants are found as insoluble particles in water [16]. The natural radionuclide content of recycled agro-industrial wastes results in environmental radiation risks due to increased exposure doses [9]. One of the key findings from the naturally occurring radioactive material (NORM) databases showed that building materials had a greater proportion of roughly 85% compared to generated wastes, which only generated an excessive gamma dose rate of 41.7%, which was less than the acceptable value (1 mSv y^{-1}) [17].

Natural radionuclides in building materials are highly active. The descendants of ^{222}Rn, such as ^{214}Pb and ^{214}Bi, are active and responsible for the dose due to their high-energy gamma emissions and ^{228}Ac and ^{208}Ti [18]. About 80% of building occupants spend their time indoors [13]. The radioactive elements in building materials and their compositions are critical in evaluating population exposures [19]. The accumulation of ^{222}Rn from the ^{238}U series, ^{220}Rn from ^{232}Th, and ^{219}Rn from ^{235}U over time, and poor ventilation might increase cancer risks in the building occupants [20]. Indoor radon levels increase with decreasing ventilation rates due to improved energy-efficient building designs [21].

Building materials possess the natural radioactive series of radionuclides, such as ^{226}Ra, ^{232}Th, ^{40}K, and ^{238}U [22]. What is used is the reservoir radionuclide, which has the longest period of the series and is easy to be in equilibrium. In the ^{238}U series, the reservoir is ^{238}U. The ^{226}Ra is used because its descendants have higher gamma emission. The descendants of ^{232}Th are more likely to be in equilibrium since the periods are shorter. These radionuclides constitute external and internal radiation exposures. The emission of gamma radionuclides in the uranium series results in external radiation. These series primarily belong to the radium ^{226}Ra decay chain segment [14]. Natural air, water, and food radionuclides

constitute the human body's internal (inhalation) radiation. The emanation of ^{222}Rn of ^{238}U series and ^{232}Th of ^{219}Rn radioactive descendants from soil and building materials and its short-lived alpha emission represents an internally exposed source through inhalation. About 40% of the total radioactivity makes up radon, indicating the most abundant source of natural radiation [14].

The United Nations Scientific Committee on the Effects of Atomic Radiation (UNSCEAR) [16] proposes a ^{40}K concentration mean of 400 Bq kg^{-1} for soil because ^{40}K is a crucial radionuclide. Its health hazard is generated by ionizing radiation of radioactive decay, resulting in cell damage and cancer induction [14]. Canadian Nuclear Safety Commission (CNSC) [23] categorizes radiation into two basic types: ionizing and non-ionizing radiation. Ionizing radiation is electromagnetic radiation interacting with host material or matter, ionizing and modifying its atoms. The major types of ionizing radiation are alpha, gamma, beta, and x-rays. Sources of ionizing radiation are natural and artificial [23]. According to UNSCEAR [16], the four primary natural radiation sources that are environmentally ionizing radiation are cosmic, terrestrial, inhalation, and ingestion. Artificial radiation is produced by human activities, such as industrial and medical activities, atmospheric testing, and nuclear explosions or accidents [23]. These radiations exist in the environment and affect humans. Non-ionizing radiation does not carry enough energy to ionize atoms or molecules [23]. Materials used in making building materials, such as sand, soil, rock, etc., have different levels of terrestrial radionuclides [24]. These terrestrial radionuclides (radioactive isotopes) constitute humans' primary sources of external and internal radiation exposure [24]. The external exposure occurs due to gamma radiation emission following the decay of ^{226}Ra, ^{232}Th, and their progenies and ^{40}K [24]. Internal exposure comes from absorption, inhalation, and indigestion of these radioactive isotopes (^{226}Ra, ^{232}Th, and ^{40}K) or their decay products through different mechanisms [25].

The global population experiences over 85% radiation due to short-lived progeny radionuclides of ^{226}Ra, ^{232}Th, and ^{40}K. These radionuclides disintegrate continuously in the built environment [16]. The inhalation of alpha and beta emitters from the radon progenies, which are not common except under certain conditions, causes the irradiation of the cells of the pulmonary system, predominantly increasing the risk of lung cancer, skin cancer, and kidney diseases [26]. The ^{222}Rn decays in the lungs into ^{210}Po and ^{214}Po, which cause cancer as they emit high-energy alpha particles. In Europe, radon inhalation results in 3–14% of all lung cancers, corresponding to 20,000 deaths annually [27]. Because of natural radioactive emissions in France, radon accounts for about 55% of the effective radiation dose [16].

Many studies have examined the radioactive contents of recycled agro-industrial waste materials used in building and construction. For instance, the activity concentrations of concrete modified with 5–15 wt. % of furnace steel slag powder (FSP), calcite powder (CP), and corncob ash (CCA) were assessed after 28 days of casting. The findings showed that FSP, CCA, and CP can be used in concrete production at a weight percentage of 5–15 in place of cement without posing radioactive risks. The concentrations varied from 4.01 ± 0.12 to 13.08 ± 0.12 Bq kg^{-1} for ^{226}Ra, 3.64 ± 0.13 to 9.93 ± 0.08 Bq kg^{-1} for ^{232}Th, and 550.37 ± 7.92 to 1166.70 ± 11.38 Bq kg^{-1} for ^{40}K compared to the control samples, which had ^{226}Ra, ^{232}Th, and ^{40}K of 19.10 ± 0.12, 7.92 ± 0.12, and 1368.51 ± 12.32 Bq kg^{-1} [28]. Using up to 35 wt. % fly ash (FA) in cement and concrete production results in average radiological parameter values within the recommended safety limits [29]. The radiological characteristics of self-compacting concrete (SCCs) incorporating FA, silica fume (SF), and ground granulated blast furnace slag (GGBFS) at 20 wt. % replacement level exhibited the highest radium equivalent activity of 89.52, 68.01, and 72.05 Bq kg^{-1} for FA, SF, and GGBFS compared to the control concrete, which had 70.86 Bq kg^{-1} [30]. However, SCCs with 20 wt. % SF had an average radon activity concentration 4.5 times lower than the control concrete. Furthermore, the radon gas emissions decreased at 5wt. % GGBFS compared to 12.5 and 20 wt. % in the concrete [31]. The activity concentrations of radiological characteristics of carbonated Portland cement mortars made with GGBFS were lower than the control samples, which had 20.10, 14.50, and 120.20 Bq kg^{-1} for the ^{226}Ra, ^{232}Th, and ^{40}K. Besides, the annual effective dose rates were equivalent to the natural background of 0.024 mSv [32]. The radiological characterization of alkali-activated construction materials containing red mud (RM), FA, and GGBFS revealed a significant increase in emanation and exhalation indexes with increased FA and GGBFS blends, and SF and GGBFS blends, whereas the GGBFS content lowered emanation and exhalation indexes [19]. Beretka and Mathew [33] examined the naturally occurring radionuclides (NORs) of Australian buildings and industrial waste materials. The results revealed that red mud and fly ash exhibited higher radioactive levels than the acceptable limits recommended for some Organization for Economic Cooperation and Development countries. The radiological hazards of building materials used to construct houses in four Punjab Province, Pakistan districts were safe for use and did not pose any significant source of radiation hazard [34].

Despite the aforementioned studies, there is a gap in the literature due to a meager investigation into the most recent analysis of the radioactive contents of various agro-industrial byproducts. Previous research revealed a little or nonexistent correlation between the activity concentrations and other radiological hazard indexes. A lot of scattered information should be gathered and organized properly after reviewing the literature. These are the motivations behind

the conduct of this research. Prior studies mostly examined the activity concentrations of industrial byproducts, with little to no understanding of agricultural byproducts. This study adds innovation by bringing the detailed radiological sources and potential effects of industrial and agricultural byproducts into the same document, focusing on their radionuclide activities (^{226}Ra, ^{232}Th, and ^{40}K) and evaluating their various radioactive risks. These contribute to (SDG) 3 (good health and well-being), SDG 11 (sustainable cities and communities), and SDG 12 (responsible consumption and production).

The radionuclide concentrations of the recycled agro-industrial waste were used to evaluate the exposure risks, and the results were compared with the globally proposed average limits. Besides, the study correlates the materials' datasets to help identify relationships between variables. The research gives the reference data for developing a radiation-monitoring system to prevent possible health risks associated with the prospective use of agro-industrial byproducts in the construction sector. It provides new techniques for reducing the radiological risks of industrial byproducts. From the radioactive protection viewpoint, this current study would help recognize risks for people residing in buildings built with these byproducts.

2 Methodology

2.1 Sampling

The samples are usually prepared, dried at room temperature, and labelled according to each sample's type. They are pulverized via an abrasion machine, homogenized, sieved with less than 3 mm size aperture, and oven-dried at 105–110 °C for about 3 h to remove the moisture content [18, 19, 28, 32, 35]. About 100 g of each homogenized sample for accurate measurement is placed in a sealed plastic container for about 60,000 s, ensuring that ^{222}Rn and its short-lived progenies attain secular equilibrium with ^{226}Ra [36].

2.1.1 Activity concentrations (S)

A gamma-ray spectrometer of a high-purity germanium (HPGe) detector (Canberra Industries, Meriden, Connecticut) is mostly used to measure the ^{226}Ra, ^{232}Th, and ^{40}K activity concentrations in the homogenized samples [19, 32]. A 100 mm thick lead shield encapsulates the detector to reduce environmental background radiation [24]. Besides, a gamma-ray spectrometer equipped with a NaI (Tl) scintillator [28, 37] and radiochemical techniques [38] are also used to estimate activity concentrations. The radiochemical separations are used at low concentrations of activity. The activity concentration of naturally occurring radioactive materials (NORMs) is determined according to Eq. (1) [36]:

$$S = \frac{N_E}{\rho \varepsilon m t} \tag{1}$$

where S is the activity concentration of NORMs (Bq kg^{-1}), N_E is the net peak area of a peak at energy E (corrected for background), ρ is the absolute transition probability of gamma-decay, $\mathcal{E}$ is the detector efficiency at energy E, m is the mass of the sample (kg), and t is the counting time of sample (s).

2.1.2 Radium equivalent activity (Ra_{eq})

The distribution of ^{226}Ra, ^{232}Th, and ^{40}K radionuclides in any material of natural origin is not uniform [24]. Radium equivalent activity, a general index, was introduced as a single index to evaluate the total activity and radiological risk of NORMs to protect the human population from radioactive hazards (safety standards). Radium equivalent activity represents the weighted sum of activity concentrations in any material, presuming that 370 Bq kg^{-1} of ^{226}Ra, 259 Bq kg^{-1} of ^{232}Th, and 4810 Bq kg^{-1} of ^{40}K produce an equal rate of gamma dose. The maximum recommendation value of Ra_{eq} (Bq kg^{-1}) in building materials corresponding to 1.5 mSv y^{-1} of annual effective dose is 370 Bqkg^{-1} [33]. The permissible range limits of radium equivalents suitable for buildings, industries, roads and bridges, and foundations are 0–370, 370–740, 740–2220, and 2220–3700 Bq kg^{-1} [33]. The limit above 3700 Bq kg^{-1} is unsuitable for any construction activity. The Ra_{eq} is determined from Eq. (2) [36]:

$$Ra_{eq} = \left(\frac{S_{Ra}}{370} + \frac{S_{Th}}{259} + \frac{S_K}{4810}\right) \times 370 = S_{Ra} + 1.43S_{Th} + 0.077S_K \quad (2)$$

where $S_{Ra,}$ $S_{Th,}$ and S_K are activity concentrations of ^{226}Ra, ^{232}Th, and ^{40}K (Bq kg^{-1}).

2.1.3 Gamma index (I_γ)

The Gamma index represents the gamma radiation hazards associated with the NORMs. As illustrated in Eq. (3), the gamma-index concentration level is proposed to determine and regulate the gamma radiation exposure originating from the NORMs. This is with an assumption that the activity concentrations produce the same gamma dose rates of 300 Bq kg^{-1} for ^{226}Ra, 200 Bq kg^{-1} for ^{232}Th, and 3000 Bq kg^{-1} for ^{40}K [11]:

$$I_\gamma = \frac{S_{Ra}}{300} + \frac{S_{Th}}{200} + \frac{S_K}{3000} \leq 1 \quad (3)$$

where $I_\gamma = 1$ as an upper limit, $I_\gamma \leq 1$ corresponds to 0.3 mSv y^{-1}[16, 22]. $I_\gamma \leq 0.5$ corresponds to 0.3 mSv y^{-1}, and $I_\gamma \leq 1$ corresponds to 1 mSv y^{-1} for bulky materials [7, 11]. $I_\gamma \leq 2$ corresponds to 0.3 mSv y^{-1}, and $I_\gamma \leq 6$ corresponds to 1 mSv y^{-1} for superficial materials with restricted use [7, 11]. Globally, using a maximum limit of $I_\gamma \leq 1$ corresponds to 1 mSvy^{-1} is prominent among countries [24]. This is the excess effective dose without considering the 50 nGy h^{-1} background (in this case, European) or UNSCEAR.

2.1.4 Alpha index (I_α)

The alpha index (I_α) evaluates the alpha radiation from radon inhalation generated from the building materials. If the activity concentration of ^{226}Ra (S_{Ra}, Bq kg^{-1}) in building materials exceeds 200 Bq kg^{-1}, the radon exhalation results in indoor radon concentration above 200 Bq m^{-3} [39]. When ^{226}Ra (S_{Ra}, Bq kg^{-1}) in building materials is below 100 Bq kg^{-1}, the radon exhalation would unlikely cause indoor radon concentration above 200 Bq m^{-3} [39]. As a result, Nordic [39] recommended exemption and upper levels for the activity concentration of ^{226}Ra (S_{Ra}, Bq kg^{-1}) in building material as 100 Bq kg^{-1} and 200 Bq kg^{-1}. The EC [11] and the International Commission on Radiological Protection (ICRP) [40] agreed with the upper limit level of 200 Bq kg^{-1}. For building materials, Table 1 presents the gamma- and alpha-index ranges (I_γ and I_α) with corresponding equivalent dose values for construction purposes [39]. The external and internal radiation hazard indexes for safe building materials are limited to the radiation dose of 1 mSv y^{-1}. The alpha index is determined by Eq. (4) [11, 18]:

$$I_\alpha = \frac{S_{Ra}}{200} \leq 1 \quad (4)$$

2.1.5 External hazard index (H_{ex})

External radiation hazard is another index that evaluates the suitability of naturally occurring radionuclides of materials [41]. Due to the naturally occurring radionuclides in building materials, external exposure to terrestrial gamma radiation creates a hazard [22]. The radioactive risk is negligible if the limit of H_{ex} is below unity, corresponding to the upper limit of Ra_{eq} of 370 Bq kg^{-1} for the safe use of building materials [16]. Equation (5) is used to calculate the H_{ex}:

$$H_{ex} = \left(\frac{S_{Ra}}{370} + \frac{S_{Th}}{259} + \frac{S_K}{4810}\right) \leq 1 \quad (5)$$

Table 1 Ranges of activity indexes and annual equivalent dose values of building materials

I_γ and I_α value	Annual equivalent dose (mSv y^{-1})	Remark
≤ 0.5	0.3	Good material
≤ 1	1	Satisfactory material
≥ 1	≥ 1	Unsuitable material

2.1.6 Internal hazard index (H_{in})

By inhaling ^{222}Rn and its short-lived offspring produced by building materials, H_{in} measures excessive alpha radiation intrinsically [33]. To make the radiation threat negligible, H_{in} must be lower than one, as shown in Eq. (6) [42]:

$$H_{in} = \left(\frac{S_{Ra}}{185} + \frac{S_{Th}}{259} + \frac{S_K}{4810}\right) \leq 1 \tag{6}$$

2.1.7 Activity utilization index (AUI)

Buildings are constructed with various naturally occurring radionuclides having activity concentrations, which strongly affect the indoor absorbed dose. The building walls absorb the outdoor radiation due to naturally occurring radionuclides in building materials, elevating the indoor dose rates. The activity utilization index, as illustrated in Eq. (7), is applied to estimate the air dose rates from various combinations of ^{226}Ra, ^{232}Th, and ^{40}K radionuclides in building materials, using appropriate conversion factors [18]:

$$AUI = \left(\frac{S_{Ra}}{50}\right)f_{Ra} + \left(\frac{S_{Th}}{50}\right)f_{Th} + \left(\frac{S_K}{500}\right)f_K \leq 1 \tag{7}$$

where $S_{Ra,}$ $S_{Th,}$ and S_K are activity concentrations of ^{226}Ra, ^{232}Th, and ^{40}K (Bq kg^{-1}); f_{Ra} (0.462), f_{Th} (0.604), and f_K (0.041) are fractional contributions to the total air dose rate attributed to gamma radiation from the activity concentrations of ^{226}Ra, ^{232}Th, and ^{40}K radionuclides. When AUI ≤ 1 corresponds to ≤ 1 mSv y^{-1} of the annual effective dose, the material can be safely used as building material [18].

2.1.8 Absorbed gamma dose rates

The gamma radiation from activity concentrations in building materials results in the absorbed dose rate exposure [16]. The maximum rate for absorbed gamma dose is 84 nGy h^{-1} [16]. This dose is determined based on the Nuccetelli et al.'s room model [43], as a common scenario.

Absorbed dose rate in outdoor exposure (AD_{out}): The absorbed dose rate in the air ($AD_{out,}$ nGy h^{-1}) via external exposure due to the gamma radiation from the ^{226}Ra, ^{232}Th, and ^{40}K radionuclides in building materials at 1 m above the ground surface can be determined by Eq. (8) [16, 33].

$$AD_{out} = 0.462SR_a + 0.604S_{Th} + 0.0417S_K \tag{8}$$

where 0.462, 0.604, and 0.0417 nGy h^{-1} per Bq kg^{-1} are the conversion coefficients of ^{226}Ra, ^{232}Th, and ^{40}K.

Absorbed dose rate in indoor exposure (AD_{in}): Recall that about 80% of building occupants spend their time indoors. Estimating the absorbed dose rate through indoor exposure is essential. As illustrated in Eq. (9), the absorbed dose rate in indoor exposure (AD_{out}, nGy h^{-1}) is 1.4 times the outdoor exposure [22]:

$$AD_{in} = 1.4 \times AD_{out} \tag{9}$$

The European Commission (EC) [11] proposed a generalized concept, as illustrated in Eq. (10), to estimate the absorbed dose rate in indoor exposure:

$$AD_{in} = 0.92SR_a + 1.10S_{Th} + 0.08S_K \tag{10}$$

The equivalent coefficients of 0.92, 1.10, and 0.08 in Eq. (10) are the conversion of activity concentration (Bq kg^{-1}) to absorbed dose rate in indoor exposure ($AD_{in,}$ nGy h^{-1}) [24].

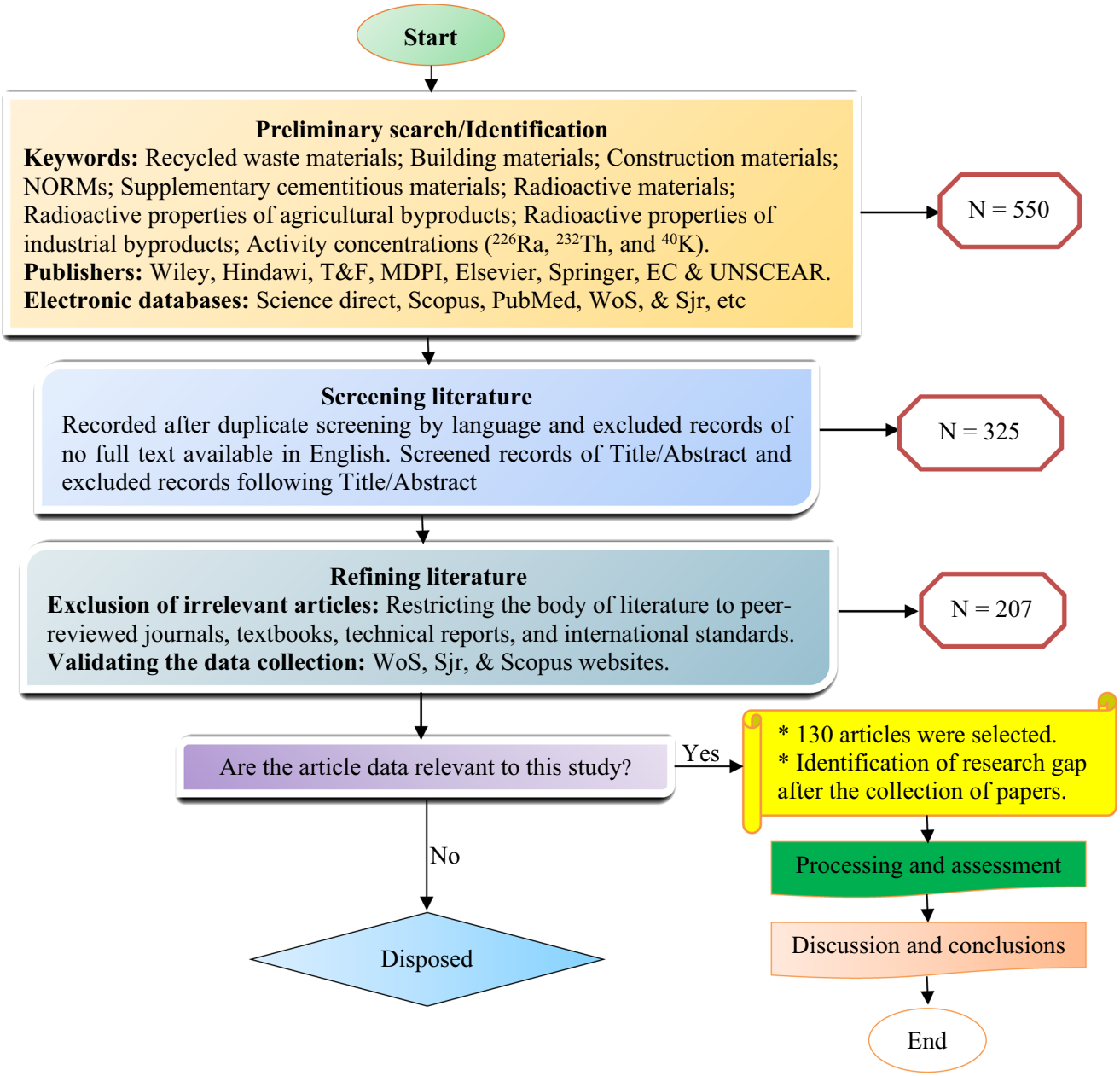

Fig. 1 A schematic flowchart of data source and collection

2.1.9 Annual effective dose rates (AED)

The annual effective dose rate measures the exposure hazard attributed to the absorbed dose [44]. The AD_{in} exposure at 1 m and AD_{out} exposure at 1.4 m above the floor level do not guarantee the radiological safety of the exposed population [45]. Consequently, the AED (mSv y^{-1}) considers the absorbed dose rates using a dose conversion factor of 0.7 sv Gy^{-1}, indoor occupancy factor of 80%, and outdoor occupancy factor of 20% [22, 46]. The annual effective dose absorbed by human beings owing to building materials is recommended to be less than 0.48 mSv y^{-1} [16, 22] or the maximum limit rate of 1 mSv y^{-1} [7].

The annual outdoor effective dose rate (AED_{out}) is determined by Eq. (11):

$$AED_{out}(mSvy^{-1}) = AD_{out} \times 24h \times 365.25d \times 0.2 \times 0.7 \times 10^{-6} = 0.00123 \times AD_{out} \quad (11)$$

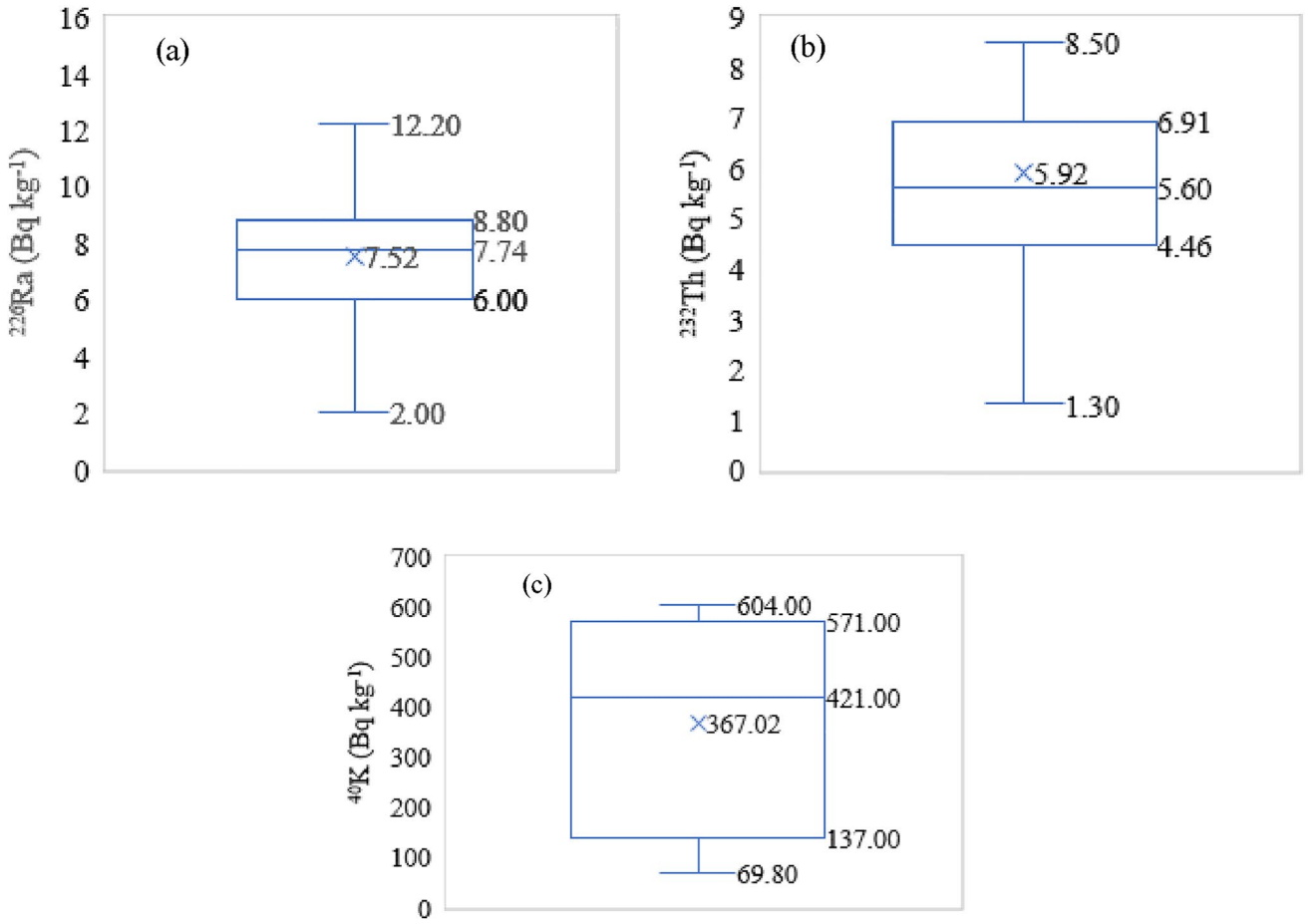

Fig. 2 Box and whisker plots for agricultural byproducts **a** ^{226}Ra, **b** ^{232}Th, and **c** ^{40}K

The annual indoor effective dose rate (AED_{in}) is evaluated by Eq. (12):

$$AED_{in}(mSvy^{-1}) = AD_{in} \times 24h \times 365.25d \times 1.4 \times 0.8 \times 0.7 \times 10^{-6} = 0.00687 \times AD_{in} \quad (12)$$

2.1.10 Excess lifetime cancer risk (ELCR)

There is a probable occurrence of cancer over a lifetime due to ionizing radiation exposure. Mutations caused by radioactivity are random, making the determination of excess lifetime cancer risk difficult, except in specific cases, to determine the type of cancer produced. Equations (13)-(15) can be applied, but with caution, to determine the ELCR [11, 24].

$$ELCR_{out} = AED_{out} \times L_S \times R_F \quad (13)$$

$$ELCR_{in} = AED_{in} \times L_S \times R_F \quad (14)$$

$$ELCR_{total} = (AED_{out} + AED_{in}) \times L_S \times R_F \quad (15)$$

where RF is the risk factor (Sv^{-1}), representing Sievert's fatal cancer risk, and LS is the life span (70 years). The detriment coefficient for stochastic impacts in ICRP 60 [47] is 5.0×10^{-2} Sv^{-1} for the entire population.

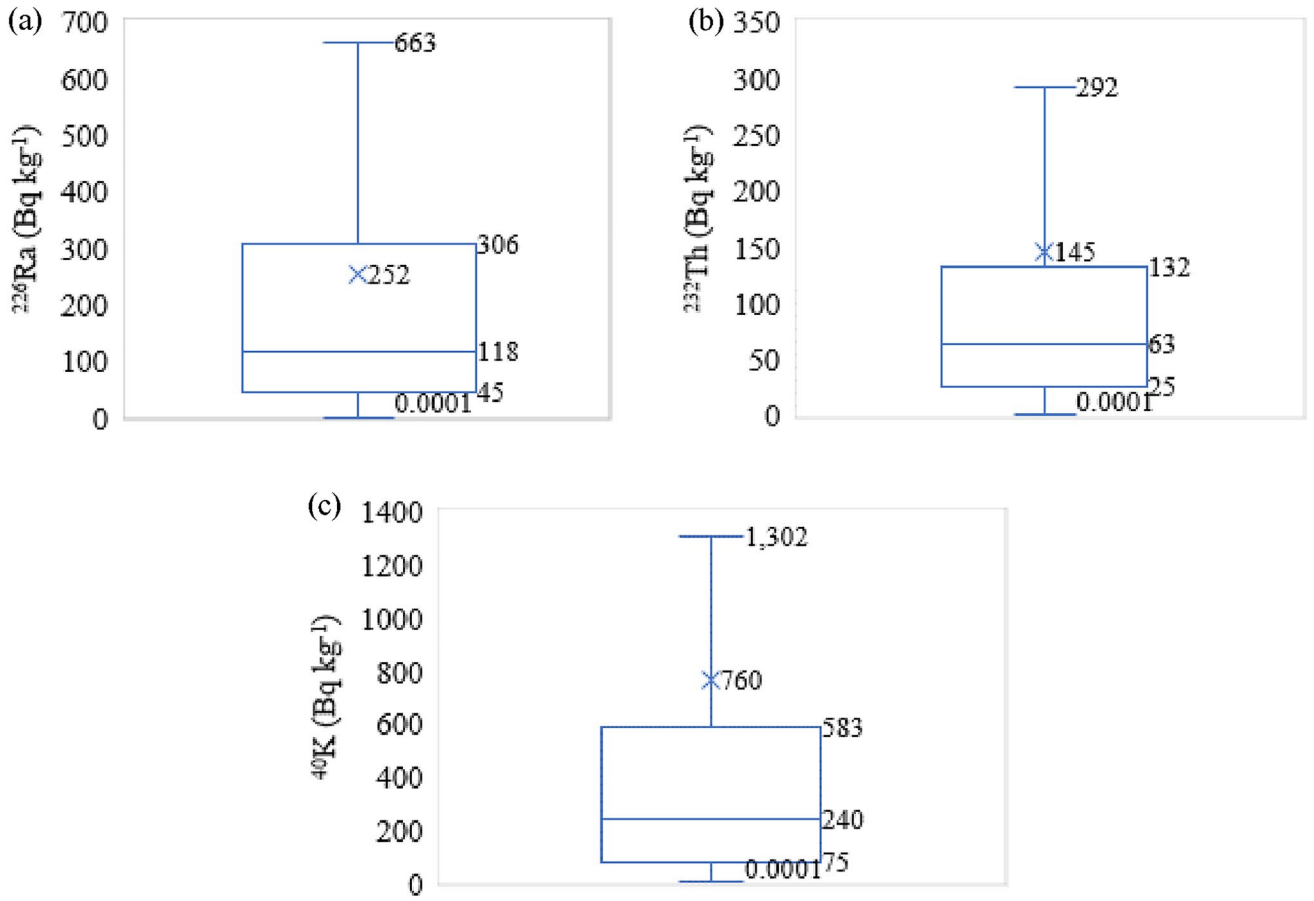

Fig. 3 Box and whisker plots for industrial byproducts **a** ^{226}Ra, **b** ^{232}Th, and **c** ^{40}K

2.2 Data source and collection

The procedure entails identification, gathering, screening, and evaluating relevant information. Data was sourced from several publishers, including Wiley, Hindawi, Taylor & Francis (T&F), Elsevier, Springer, and Multidisciplinary Digital Publishing Institute (MDPI), etc. The references were restricted to databases like Web of Science (WoS), Scimago Journal & Country Rank (Sjr), and Scopus websites to ensure that only peer-reviewed references were included and to validate the data collection. To broaden the scope of data collection, relevant data was acquired from EC and UNSCEAR. The screening was done while keeping in mind the importance of the study and concentrating on the concentration of activities of recycled agro-industrial waste materials. A total of 550 peer-reviewed papers were obtained based on the preliminary search. However, a sample size of 325 pertinent peer-reviewed papers was collected after screening. Thereafter, the papers were carefully selected, researched, examined, and read to investigate, validate, and control duplicity. After a thorough refinement, a sample size of 207 suitable articles was identified for the study. Finally, a data size of 130 peer-reviewed publications was relevant and considered for the research. Figure 1 presents the methodological flowchart for data source and collection.

2.2.1 Data classification

The data are classified into two groups: agricultural and industrial byproducts.

Agricultural byproducts. The agricultural byproducts surveyed by this research were rice husk ash (RHA), mussel shell (MS), palm oil clinker (POC), and palm oil fuel ash (POFA).

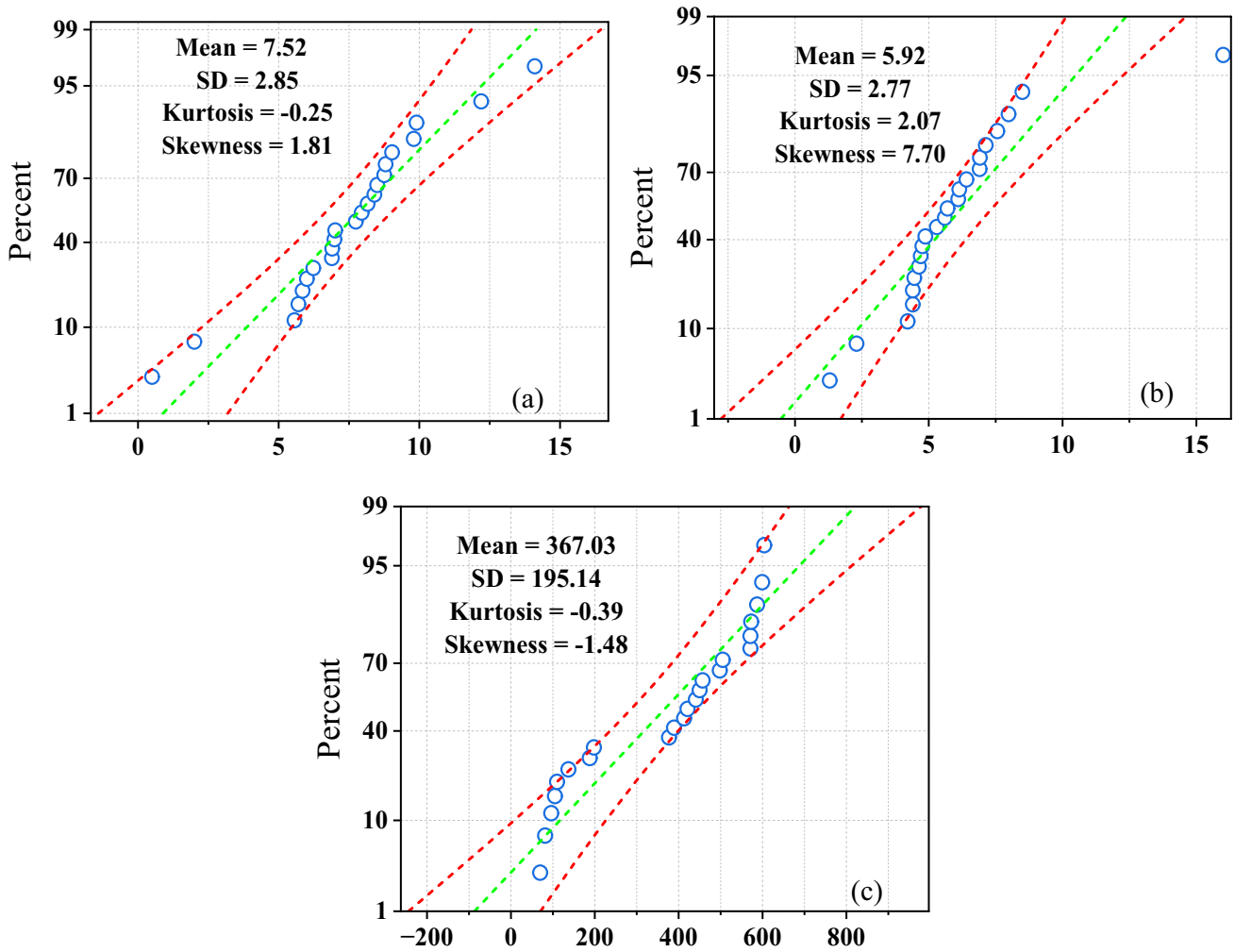

Fig. 4 Normal probability plots for agricultural byproducts of **a** ^{226}Ra, **b** ^{232}Th, and **c** ^{40}K

Industrial byproducts. The industrial byproducts considered in this study were bottom ash (BA), biomass ash (BA), copper slag (CS), fly ash (FA), ground granulated blast furnace slag (GGBFS), granite waste powder (GWP), incinerated sewage sludge ash (ISSA), lead slag (LS), metakaolin (MK), marble powder (MP), mill tailings (MT), nickel slag (NS), pyrite ash (PA), phosphogypsum (PG), Pumice (PM). Others were red mud/bauxite residue (RM), silica fume (SF), steel slag (SS), tin slag (TS), volcanic ash (VA), and waste glass powder (WP).

2.2.2 Statistical analysis

(a)(a) Box and whisker analysis

A Minitab statistical software version 18.1 was used to perform the Box and Whisker analysis. A box and whisker analysis, also called a box plot, is a graphical method used to visually represent the distribution of data by showing the spread, central tendency (median), and potential outliers within a dataset, allowing for easy comparison between different groups of data through a compact summary of key statistics like minimum, maximum, first quartile, and third quartile. Box and whisker plots combine data from various sources and display the findings in a single graph, making them incredibly efficient and simple to read. A box and whisker plot displays the five-number summary of a data set. The five-number summary includes the minimum, first quartile, second quartile (median), third quartile, and maximum. From Fig. 2a, the minimum and maximum whisker values were 2.00 and 12.20 Bq kg^{-1}, while 7.74 and 7.52 Bq kg^{-1} showed box

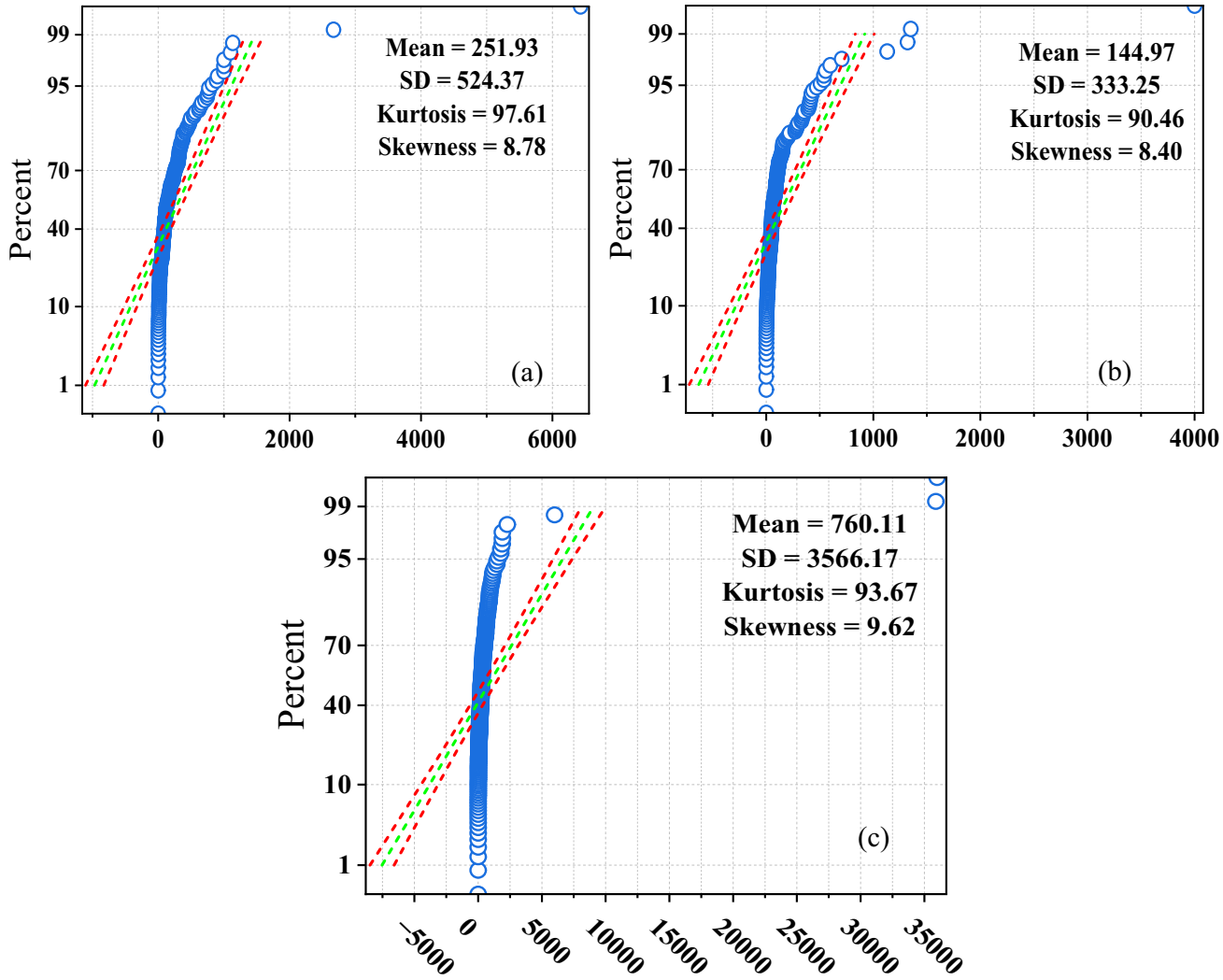

Fig. 5 Normal probability plots for industrial byproducts of **a** ^{226}Ra, **b** ^{232}Th, and **c** ^{40}K

Table 2 Activity concentrations and radiological evaluation of rice husk ash (RHA)

Activity concentration					Radiological evaluation using Eqs. (2–15)												
Material	S (Bq kg^{-1})			References	Ra_{eq} (Bq kg^{-1})	I_γ	I_α	H_{ex}	H_{in}	AUI	AD (nGy h^{-1})		AED (mSv y^{-1})		ELCR ($\times 10^{-3}$)		
	^{226}Ra	^{232}Th	^{40}K								Out	In	Out	In	Out	In	Total
RHA	6	16	505	[19]	68	0.27	0.03	0.18	0.20	0.29	33	47	0.041	0.32	0.14	1.13	1.27
Average	6	16	505		68	0.27	0.03	0.18	0.20	0.29	33	47	0.041	0.32	0.14	1.13	1.27
UNSCEAR	33	45	420	[22, 46]	370	≤ 1	≤ 1	≤ 1	≤ 1	≤ 1	59	84	0.07	0.41	0.29	1.16	1.45

*UNSCEAR: United Nations Scientific Committee on the Effects of Atomic Radiation (World Population-Weighted Average Value)

median and mean. Outliers, though, appeared in MS at 14.10 and 0.50 Bq kg^{-1}. Similar trends were observed in the ^{232}Th series, where the box median and mean were 5.60 and 5.92 Bq kg^{-1} in Fig. 2b, but at 16.00 Bq kg^{-1}, RHA showed an outlier. The ^{40}K isotope shown in Fig. 2c showed the box median and mean of 412 and 367.02 Bq kg^{-1} without the influence of an outlier. Figure 3a shows statistics for the ^{226}Ra series of industrial byproducts, with median and mean values of 118 and 252 Bq kg^{-1} and outliers ranging from 710 to 6,248 Bq kg^{-1}. The median and mean values for the ^{232}Th series, shown in Fig. 3b, are 63 and 145 Bq kg^{-1}. There were outliers, ranging from 300 to 4,000 Bq kg^{-1}. For the ^{40}K isotopes depicted

Table 3 Activity concentrations and radiological evaluation of mussel shell (MS)

Activity concentration					Radiological evaluation using Eqs. (2–15)												
Material	S (Bq kg^{-1})			References	Ra_{eq} (Bq kg^{-1})	I_γ	I_α	H_{ex}	H_{in}	AUI	AD (nGy h^{-1})		AED (mSv y^{-1})		ELCR ($\times 10^{-3}$)		
	^{226}Ra	^{232}Th	^{40}K								Out	In	Out	In	Out	In	Total
MS	14.1	8.5	137	[56]	37	0.14	0.07	0.10	0.14	0.24	17	24	0.021	0.17	0.07	0.58	0.66
MS	9.9	6.1	96.2	[56]	26	0.10	0.05	0.07	0.00	0.17	12	17	0.015	0.12	0.05	0.41	0.47
MS	9.8	5.7	69.8	[56]	23	0.08	0.05	0.06	0.09	0.17	11	15	0.013	0.10	0.05	0.37	0.41
MS	12.2	5.6	110	[56]	29	0.11	0.06	0.08	0.11	0.19	14	19	0.017	0.13	0.06	0.46	0.52
MS	8.8	5.3	105	[56]	24	0.09	0.04	0.07	0.09	0.15	12	16	0.014	0.11	0.05	0.39	0.44
MS	8.4	4.4	81.4	[56]	21	0.08	0.04	0.06	0.08	0.14	10	14	0.012	0.10	0.04	0.33	0.38
MS	0.5	1.3	198	[57]	18	0.07	0.00	0.05	0.05	0.04	9	13	0.011	0.09	0.04	0.31	0.35
MS	8.5	4.7	389	[57]	45	0.18	0.04	0.12	0.14	0.17	23	32	0.028	0.22	0.10	0.77	0.87
MS	2.0	2.3	188	[57]	20	0.08	0.01	0.05	0.06	0.06	10	14	0.012	0.10	0.04	0.34	0.39
MS	5.7	6.9	377	[57]	45	0.18	0.03	0.12	0.14	0.17	23	32	0.028	0.22	0.10	0.76	0.86
Average	7.99	5.08	175		29	0.11	0.04	0.08	0.09	0.15	14	20	0.017	0.14	0.06	0.47	0.54
UNSCEAR	33	45	420	[22, 46]	370	≤ 1	≤ 1	≤ 1	≤ 1	≤ 1	59	84	0.07	0.41	0.29	1.16	1.45

Table 4 Activity concentrations and radiological evaluation of palm oil clinker (POC)

Activity concentration					Radiological evaluation using Eqs. (2–15)												
Material	S (Bq kg^{-1})			References	Ra_{eq} (Bq kg^{-1})	I_γ	I_α	H_{ex}	H_{in}	AUI	AD (nGy h^{-1})		AED (mSv y^{-1})		ELCR ($\times 10^{-3}$)		
	^{226}Ra	^{232}Th	^{40}K								Out	In	Out	In	Out	In	Total
POC	6.89	4.46	571	[57]	57	0.24	0.03	0.15	0.17	0.16	29	41	0.037	0.20	0.13	1.00	1.13
POC	6.90	4.63	571	[57]	57	0.24	0.03	0.15	0.17	0.17	29	41	0.037	0.20	0.13	1.00	1.13
POC	5.85	4.40	573	[57]	56	0.24	0.03	0.15	0.17	0.15	29	40	0.036	0.19	0.13	0.98	1.11
POC	7.01	4.87	599	[57]	60	0.24	0.04	0.16	0.18	0.17	31	43	0.038	0.30	0.13	1.05	1.18
POC	5.56	4.21	604	[57]	58	0.24	0.02	0.16	0.17	0.15	30	42	0.037	0.29	0.13	1.02	1.15
POC	6.23	4.76	587	[57]	58	0.24	0.03	0.16	0.17	0.16	30	42	0.037	0.29	0.13	1.02	1.15
Average	6.41	4.56	584		58	0.24	0.03	0.16	0.17	0.16	30	42	0.04	0.25	0.13	1.01	1.14
UNSCEAR	33	45	420	[22, 46]	370	≤ 1	≤ 1	≤ 1	≤ 1	≤ 1	59	84	0.07	0.41	0.29	1.16	1.45

Table 5 Activity concentrations and radiological evaluation of palm oil fuel ash (POFA)

Activity concentration					Radiological evaluation using Eqs. (2–15)												
Material	S (Bq kg^{-1})			References	Ra_{eq} (Bq kg^{-1})	I_γ	I_α	H_{ex}	H_{in}	AUI	AD (nGy h^{-1})		AED (mSv y^{-1})		ELCR ($\times 10^{-3}$)		
	^{226}Ra	^{232}Th	^{40}K								Out	In	Out	In	Out	In	Total
POFA	8.16	6.14	441	[57]	51	0.20	0.04	0.14	0.16	0.19	26	36	0.032	0.25	0.11	0.87	0.98
POFA	7.74	6.41	450	[57]	52	0.21	0.04	0.14	0.16	0.19	26	36	0.032	0.25	0.11	0.88	1.00
POFA	7.95	7.13	457	[57]	53	0.21	0.04	0.14	0.17	0.20	27	38	0.033	0.26	0.12	0.91	1.03
POFA	8.75	7.98	421	[57]	53	0.21	0.04	0.16	0.18	0.21	26	37	0.032	0.25	0.11	0.89	1.00
POFA	9.03	7.56	498	[57]	58	0.23	0.05	0.13	0.15	0.22	29	41	0.036	0.28	0.13	0.99	1.12
POFA	6.98	6.91	413	[57]	49	0.19	0.03	0.14	0.16	0.18	24	34	0.030	0.24	0.11	0.83	0.93
Average	8.10	7.02	447		53	0.21	0.04	0.14	0.16	0.20	26	37	0.030	0.26	0.12	0.90	1.01
UNSCEAR	33	45	420	[22, 46]	370	≤ 1	≤ 1	≤ 1	≤ 1	≤ 1	59	84	0.07	0.41	0.29	1.16	1.45

Table 6 Activity concentrations and radiological evaluation of bottom ash (BA)

Activity concentration					Radiological evaluation using Eqs. (2–15)												
Material	S (Bq kg^{-1})			References	Ra_{eq} (Bq kg^{-1})	I_γ	I_α	H_{ex}	H_{in}	AUI	AD (nGy h^{-1})		AED (mSv y^{-1})		ELCR ($\times 10^{-3}$)		
	^{226}Ra	^{232}Th	^{40}K								Out	In	Out	In	Out	In	Total
BA	306	65	233	[19]	417	1.42	1.53	1.13	1.95	3.63	190	266	0.23	1.83	0.82	6.41	7.23
BA	113	68	623	[19]	258	0.92	0.57	0.70	1.00	1.92	119	167	0.15	1.15	0.51	4.01	4.53
BA	345	59	410	[17]	461	1.58	1.73	1.25	2.18	3.93	212	297	0.26	2.04	0.91	7.14	8.05
BA	423	35	296	[63]	496	1.68	2.12	1.34	2.48	4.36	229	320	0.28	2.20	0.99	7.71	8.69
BA	139	108	292	[64]	316	1.10	0.70	0.85	1.23	2.61	142	198	0.17	1.36	0.61	4.77	5.38
BA	56	63	210	[65]	162	0.57	0.28	0.44	0.59	1.30	73	102	0.09	0.70	0.31	2.45	2.76
BA	62	53	457	[66]	173	0.62	0.31	0.47	0.63	1.25	80	112	0.10	0.77	0.34	2.68	3.03
BA	663	44	397	[67]	756	2.56	3.32	2.04	3.84	6.69	349	489	0.43	3.36	1.50	11.76	13.27
BA	114	124	210	[68]	307	1.07	0.57	0.83	1.14	2.57	136	191	0.17	1.31	0.59	4.59	5.18
BA	100	105	132	[69]	260	0.90	0.50	0.70	0.97	2.20	115	161	0.14	1.11	0.50	3.88	4.37
BA	94	105	272	[70]	265	0.93	0.47	0.72	0.97	2.16	118	165	0.15	1.14	0.51	3.98	4.49
BA	70	40	355	[71]	155	0.55	0.35	0.42	0.61	1.16	71	100	0.09	0.69	0.31	2.40	2.71
BA	108	79	514	[72]	261	0.93	0.54	0.70	1.00	1.99	119	167	0.15	1.14	0.51	4.01	4.52
BA	541	102	714	[73]	742	2.55	2.71	2.00	3.47	6.29	341	478	0.42	3.28	1.47	11.49	12.96
BA	68	74	225	[74]	191	0.67	0.34	0.52	0.70	1.54	85	120	0.11	0.82	0.37	2.88	3.25
BA	70	64	457	[59]	197	0.71	0.35	0.53	0.72	1.46	90	126	0.11	0.87	0.39	3.03	3.42
BA	66	97	170	[75]	218	0.76	0.33	0.59	0.77	1.80	96	135	0.12	0.92	0.41	3.24	3.65
Average	196	76	351		331	1.15	0.98	0.90	1.43	2.76	151	211	0.19	1.45	0.65	5.08	5.73
UNSCEAR	33	45	420	[22, 46]	370	≤ 1	≤ 1	≤ 1	≤ 1	≤ 1	59	84	0.07	0.41	0.29	1.16	1.45

Table 7 Activity concentrations and radiological evaluation of biomass ash (BM)

Activity concentration					Radiological evaluation using Eqs. (2–15)												
Material	S (Bq kg^{-1})			References	Ra_{eq} (Bq kg^{-1})	I_γ	I_α	H_{ex}	H_{in}	AUI	AD (nGy h^{-1})		AED (mSv y^{-1})		ELCR ($\times 10^{-3}$)		
	^{226}Ra	^{232}Th	^{40}K								Out	In	Out	In	Out	In	Total
BM	12	7	36,000	[76]	2,794	12.1	0.06	7.54	7.58	3.15	1511	2115	1.86	14.5	6.50	50.86	57.37
BM	10	6	6,000	[76]	481	2.1	0.05	1.30	1.32	0.66	258	362	0.32	2.5	1.11	8.70	9.81
BM	9	4	35,898	[2]	2,779	12.0	0.05	7.50	7.53	3.08	1504	2105	1.85	14.5	6.47	50.61	57.09
Average	10	6	25,966		2,018	8.7	0.05	5.00	5.00	2.00	1091	1527	1.00	10.5	5.00	37.00	41.00
UNSCEAR	33	45	420	[22, 46]	370	≤ 1	≤ 1	≤ 1	≤ 1	≤ 1	59	84	0.07	0.41	0.29	1.16	1.45

in Fig. 3c, the median and mean values were 240 and 760 Bq kg^{-1}. Outliers ranging from 1,463 to 35,898 Bq kg^{-1} were the outcome. The outlier results could be explained by variations in the region and industry that produced these agro-industrial byproducts, which would impact the sample data's box median and mean.

(b)(b) Normal probability analysis

OriginPro 2024b version 10.1.5.132 was engaged to perform the normal probability analysis. The normal probability plot is a graphical technique for assessing whether or not a data set is approximately normally distributed. It plots the quantiles of the dataset against the quantiles of a standard normal distribution. The data is said to be normally distributed if the data points approximately follow a straight line; if not, it indicates a non-normality. Outliers indicate points at the ends of the line that are far from the rest of the data. An S-curve pattern indicates that the data is skewed, with one tail longer than the other [48]. The effects of dataset distribution characteristics are displayed in Figs. 4 and 5. For the purpose of risk exposure

Table 8 Activity concentrations and radiological evaluation of copper slag (CS)

Activity concentration					Radiological evaluation using Eqs. (2–15)												
Material	S (Bq kg^{-1})			References	Ra_{eq} (Bq kg^{-1})	I_γ	I_α	H_{ex}	H_{in}	AUI	AD (nGy h^{-1})		AED (mSv y^{-1})		ELCR ($\times 10^{-3}$)		
	^{226}Ra	^{232}Th	^{40}K								Out	In	Out	In	Out	In	Total
CS	1135	50	585	[73]	1,252	4.23	5.68	3.38	6.45	11.1	579	811	0.71	5.57	2.49	19.49	21.98
CS	770	52	650	[73]	894	3.04	3.85	2.42	4.50	7.80	414	580	0.51	3.98	1.78	13.94	15.73
CS	317	54	886	[73]	462	1.62	1.59	1.25	2.11	3.65	216	302	0.27	2.08	0.93	7.27	8.20
CS	317	54	887	[77]	463	1.62	1.59	1.25	2.11	3.65	216	302	0.27	2.08	0.93	7.27	8.20
CS	770	52	650	[78]	894	3.04	3.85	2.42	4.50	7.80	414	580	0.51	3.98	1.78	13.94	15.73
Average	662	52	732		793	3.00	3.00	2.00	4.00	7.00	368	515	0.00	4.00	2.00	12.00	14.00
UNSCEAR	33	45	420	[22, 46]	370	≤ 1	≤ 1	≤ 1	≤ 1	≤ 1	59	84	0.07	0.41	0.29	1.16	1.45

Table 9 Activity concentrations and radiological evaluation of fly ash (FA)

Activity concentration					Radiological evaluation using Eqs. (2–15)												
Material	S (Bq kg^{-1})			References	Ra_{eq} (Bq kg^{-1})	I_γ	I_α	H_{ex}	H_{in}	AUI	AD (nGy h^{-1})		AED (mSv y^{-1})		ELCR ($\times 10^{-3}$)		
	^{226}Ra	^{232}Th	^{40}K								Out	In	Out	In	Out	In	Total
FA	119	91	438	[54]	283	1.00	0.60	0.76	1.09	2.23	128	179	0.16	1.23	0.55	4.32	4.87
FA	78	126	374	[66]	287	1.01	0.39	0.78	0.99	2.27	128	179	0.16	1.23	0.55	4.30	4.85
FA	904	53	454	[67]	1,015	3.43	4.52	2.74	5.19	9.03	469	656	0.58	4.51	2.02	15.8	17.79
FA	100	108	388	[76]	284	1.00	0.50	0.77	1.04	2.26	128	179	0.16	1.23	0.55	4.30	4.85
FA	88	88	868	[79]	281	1.02	0.44	0.76	1.00	1.95	130	182	0.16	1.25	0.56	4.38	4.94
FA	188	91	343	[73]	345	1.20	0.94	0.93	1.44	2.86	156	219	0.19	1.50	0.67	5.26	5.93
FA	999	200	1,100	[73]	1,370	4.70	5.00	3.70	6.40	11.7	628	879	0.77	6.04	2.70	21.2	23.85
FA	191	91	561	[17]	364	1.28	0.96	0.98	1.50	2.91	167	233	0.20	1.60	0.72	5.61	6.33
FA	232	117	466	[80]	435	1.51	1.16	1.18	1.80	3.60	197	276	0.24	1.90	0.85	6.64	7.49
FA	825	53	402	[63]	932	3.15	4.13	2.52	4.75	8.30	430	602	0.53	4.14	1.85	14.5	16.32
FA	45	40	88	[81]	109	0.38	0.23	0.29	0.42	0.91	49	68	0.06	0.47	0.21	1.64	1.85
FA	126	89	793	[82]	314	1.13	0.63	0.85	1.19	2.30	145	203	0.18	1.39	0.62	4.88	5.51
FA	14	20	1,148	[71]	131	0.53	0.07	0.35	0.39	0.47	66	93	0.08	0.64	0.29	2.24	2.52
FA	41	49	321	[83]	136	0.49	0.21	0.37	0.48	1.00	62	87	0.08	0.60	0.27	2.08	2.35
FA	99	113	309	[84]	284	1.00	0.50	0.77	1.04	2.31	127	178	0.16	1.22	0.55	4.27	4.82
FA	139	82	743	[19]	313	1.12	0.70	0.85	1.22	2.34	145	203	0.18	1.39	0.62	4.87	5.50
FA	83	87	235	[65]	226	0.79	0.42	0.61	0.83	1.84	101	141	0.12	0.97	0.43	3.39	3.82
FA	70	79	233	[65]	201	0.71	0.35	0.54	0.73	1.62	90	126	0.11	0.86	0.39	3.02	3.41
FA	100	180	650	[11]	407	1.45	0.50	1.10	1.37	3.15	182	255	0.22	1.75	0.78	6.13	6.91
FA	80	207	546	[85]	418	1.48	0.40	1.13	1.35	3.28	185	259	0.23	1.78	0.80	6.22	7.01
FA	90	66	240	[9]	203	0.71	0.45	0.55	0.79	1.65	91	128	0.11	0.88	0.39	3.08	3.47
FA	999	56	470	[86]	1,115	3.77	5.00	3.01	5.71	9.95	515	721	0.63	4.95	2.22	17.4	19.55
FA	161	156	584	[86]	429	1.51	0.81	1.16	1.59	3.42	193	270	0.24	1.86	0.83	6.50	7.33
FA	119	147	352	[87]	356	1.25	0.60	0.96	1.28	2.90	158	222	0.19	1.52	0.68	5.33	6.02
FA	118	157	1,463	[88]	455	1.67	0.59	1.23	1.55	3.11	210	294	0.26	2.02	0.91	7.08	7.99
FA	441	110	510	[89]	638	2.19	2.21	1.72	2.91	5.45	291	408	0.36	2.80	1.25	9.81	11.07
FA	242	31	382	[90]	316	1.09	1.21	0.85	1.51	2.64	146	205	0.18	1.41	0.63	4.93	5.56
FA	263	49	216	[90]	350	1.19	1.32	0.94	1.66	3.04	160	224	0.20	1.54	0.69	5.39	6.08
FA	143	117	719	[59]	366	1.30	0.72	0.99	1.37	2.79	167	233	0.21	1.60	0.72	5.61	6.33
FA	75	104	1,030	[75]	303	1.11	0.38	0.82	1.02	2.03	140	197	0.17	1.35	0.60	4.73	5.33
Average	239	99	548		422	1.00	1.00	1.00	2.00	3.00	193	270	0.24	2.00	1.00	6.00	7.00
UNSCEAR	33	45	420	[22, 46]	370	≤ 1	≤ 1	≤ 1	≤ 1	≤ 1	59	84	0.07	0.41	0.29	1.16	1.45

Table 10 Activity concentrations and radiological evaluation of ground granulated blast furnace slag (GGBFS)

Activity concentration					Radiological evaluation using Eqs. (2–15)												
Material	S (Bq kg^{-1})			References	Ra_{eq} (Bq kg^{-1})	I_γ	I_α	H_{ex}	H_{in}	AUI	AD (nGy h^{-1})		AED (mSv y^{-1})		ELCR ($\times 10^{-3}$)		
	^{226}Ra	^{232}Th	^{40}K								Out	In	Out	In	Out	In	Total
GGBFS	112	52	205	[91]	202	0.70	0.56	0.55	0.85	1.68	92	128	0.11	0.88	0.39	3.09	3.48
GGBFS	182	44	269	[19]	266	0.92	0.91	0.72	1.21	2.24	122	171	0.15	1.17	0.52	4.10	4.63
GGBFS	179	55	172	[19]	271	0.93	0.90	0.73	1.22	2.33	123	172	0.15	1.18	0.53	4.14	4.67
GGBFS	128	45	119	[19]	202	0.69	0.64	0.54	0.89	1.74	91	128	0.11	0.88	0.39	3.07	3.47
GGBFS	89	140	378	[66]	318	1.12	0.45	0.86	1.10	2.54	141	198	0.17	1.36	0.61	4.76	5.37
GGBFS	151	150	14	[76]	367	1.26	0.76	0.99	1.40	3.21	161	225	0.20	1.55	0.69	5.42	6.11
GGBFS	143	163	15	[76]	377	1.30	0.72	1.02	1.41	3.29	165	231	0.20	1.59	0.71	5.56	6.27
GGBFS	98	89	96	[76]	233	0.80	0.49	0.63	0.89	1.99	103	144	0.13	0.99	0.44	3.47	3.91
GGBFS	34	44	846	[76]	162	0.62	0.17	0.44	0.53	0.92	78	109	0.10	0.75	0.33	2.61	2.94
GGBFS	32	35	632	[76]	131	0.49	0.16	0.35	0.44	0.77	62	87	0.08	0.60	0.27	2.10	2.36
GGBFS	97	89	96	[79]	232	0.80	0.49	0.63	0.89	1.98	103	144	0.13	0.99	0.44	3.45	3.89
GGBFS	251	25	362	[73]	315	1.08	1.26	0.85	1.53	2.65	146	205	0.18	1.41	0.63	4.92	5.55
GGBFS	323	40	158	[73]	392	1.33	1.62	1.06	1.93	3.48	180	252	0.22	1.73	0.77	6.06	6.83
GGBFS	100	100	500	[73]	282	1.00	0.50	0.76	1.03	2.17	127	178	0.16	1.23	0.55	4.29	4.84
GGBFS	166	48	232	[17]	253	0.87	0.83	0.68	1.13	2.13	115	162	0.14	1.11	0.50	3.88	4.38
GGBFS	184	135	283	[17]	399	1.38	0.92	1.08	1.57	3.35	178	250	0.22	1.72	0.77	6.00	6.77
GGBFS	15	1	20	[17]	18	0.06	0.08	0.05	0.09	0.15	8	12	0.01	0.08	0.04	0.28	0.32
GGBFS	336	152	786	[17]	614	2.14	1.68	1.66	2.57	5.01	280	392	0.34	2.69	1.20	9.42	10.62
GGBFS	43	43	76	[92]	110	0.38	0.22	0.30	0.41	0.92	49	69	0.06	0.47	0.21	1.65	1.86
GGBFS	178	148	243	[80]	408	1.41	0.89	1.10	1.58	3.45	182	254	0.22	1.75	0.78	6.12	6.90
GGBFS	67	78	145	[81]	190	0.66	0.34	0.51	0.69	1.57	84	118	0.10	0.81	0.36	2.83	3.19
GGBFS	150	65	142	[71]	254	0.87	0.75	0.69	1.09	2.18	114	160	0.14	1.10	0.49	3.85	4.35
GGBFS	35	30	75	[2]	84	0.29	0.18	0.23	0.32	0.69	37	52	0.05	0.36	0.16	1.26	1.42
GGBFS	160	100	250	[2]	322	1.12	0.80	0.87	1.30	2.71	145	203	0.18	1.39	0.62	4.87	5.50
GGBFS	270	70	240	[11]	389	1.33	1.35	1.05	1.78	3.36	177	248	0.22	1.70	0.76	5.96	6.72
GGBFS	251	25	214	[93]	303	1.03	1.26	0.82	1.50	2.64	140	196	0.17	1.35	0.60	4.71	5.31
GGBFS	117	78	176	[94]	242	0.84	0.59	0.65	0.97	2.04	109	152	0.13	1.04	0.47	3.65	4.12
GGBFS	115	36	229	[95]	184	0.64	0.58	0.50	0.81	1.52	84	118	0.10	0.81	0.36	2.84	3.21
GGBFS	115	35	192	[77]	180	0.62	0.58	0.49	0.80	1.50	82	115	0.10	0.79	0.35	2.77	3.12
GGBFS	166	48	232	[96]	253	0.87	0.83	0.68	1.13	2.13	115	162	0.14	1.11	0.50	3.88	4.38
Average	143	72	247		265	0.92	0.71	0.72	1.10	2.21	120	168	0.15	1.15	0.52	4.03	4.55
UNSCEAR	33	45	420	[22, 46]	370	≤ 1	≤ 1	≤ 1	≤ 1	≤ 1	59	84	0.07	0.41	0.29	1.16	1.45

analysis, this study used raw data from pertinent literature; hence, normality is not a primary concern; rather, the probability of data values to risk levels is important. Almost all data points of activity concentrations, as shown in Fig. 4a–c for agricultural byproducts, aligned within the 95% confidence interval of the mean reference line at a 0.05 significance level. Besides, skewness and kurtosis were within the acceptable ranges of −3 and + 3 and − 10 to + 10 [49]. This indicates that there is no likelihood of risk exposure from recycled agricultural waste. However, Fig. 5a–c indicate positive asymmetry and a heavier tail from the mean reference line. This suggests that there is a likelihood of risk exposure from recycled industrial waste. It is important to state the outliers were not removed because it is challenging to gather widely distributed datasets of activity concentrations that contain industrial and agricultural outputs. Additionally, within the radiological domain, these outliers carry important information.

Table 11 Activity concentrations and radiological evaluation of granite waste powder (GWP)

Activity concentration					Radiological evaluation using Eqs. (2–15)												
Material	S (Bq kg^{-1})			References	Ra_{eq} (Bq kg^{-1})	I_γ	I_α	H_{ex}	H_{in}	AUI	AD (nGy h^{-1})		AED (mSv y^{-1})		ELCR ($\times 10^{-3}$)		
	^{226}Ra	^{232}Th	^{40}K								Out	In	Out	In	Out	In	Total
GWP	10	10	299	[97]	47	0.18	0.05	0.13	0.15	0.24	23	32	0.03	0.22	0.10	0.78	0.88
GWP	19	18	956	[97]	118	0.47	0.10	0.32	0.37	0.47	60	83	0.07	0.57	0.26	2.00	2.26
GWP	55	41	398	[60]	144	0.52	0.28	0.39	0.54	1.04	67	93	0.08	0.64	0.29	2.25	2.54
GWP	378	154	2,285	[60]	774	2.79	1.89	2.09	3.11	5.54	363	508	0.45	3.49	1.56	12.22	13.78
GWP	61	48	349	[60]	157	0.56	0.31	0.42	0.59	1.17	72	100	0.09	0.69	0.31	2.41	2.72
GWP	886	292	1,878	[60]	1,448	5.04	4.43	3.91	6.31	11.9	664	930	0.82	6.39	2.86	22.35	25.21
GWP	71	96	368	[60]	237	0.84	0.36	0.64	0.83	1.85	106	149	0.13	1.02	0.46	3.57	4.03
GWP	547	399	1,768	[60]	1,254	4.41	2.74	3.39	4.86	10.0	567	794	0.70	5.46	2.44	19.10	21.54
GWP	9	1	2	[98]	11	0.04	0.05	0.03	0.05	0.10	5	7	0.01	0.05	0.02	0.16	0.18
GWP	494	157	1,776	[98]	855	3.02	2.47	2.31	3.65	6.61	397	556	0.49	3.82	1.71	13.37	15.08
GWP	4	15	24	[99]	27	0.10	0.02	0.07	0.08	0.22	12	17	0.01	0.11	0.05	0.40	0.45
GWP	91	70	1,302	[99]	291	1.09	0.46	0.79	1.03	1.79	139	194	0.17	1.33	0.60	4.67	5.26
GWP	2	1	49	[100]	7	0.03	0.01	0.02	0.02	0.03	4	5	0.00	0.03	0.02	0.12	0.14
GWP	170	354	1,592	[100]	799	2.87	0.85	2.16	2.62	5.98	359	502	0.44	3.45	1.54	12.08	13.62
GWP	34	46	944	[101]	172	0.66	0.17	0.47	0.56	0.95	83	116	0.10	0.80	0.36	2.79	3.15
GWP	31	45	856	[101]	161	0.61	0.16	0.44	0.52	0.90	77	108	0.09	0.74	0.33	2.60	2.93
GWP	10	29	911	[101]	122	0.48	0.05	0.33	0.36	0.52	60	84	0.07	0.58	0.26	2.02	2.28
GWP	12	37	742	[101]	122	0.47	0.06	0.33	0.36	0.62	59	82	0.07	0.57	0.25	1.98	2.23
GWP	18	64	990	[101]	186	0.71	0.09	0.50	0.55	1.02	88	124	0.11	0.85	0.38	2.97	3.35
Average	153	99	920		365	1.31	0.76	0.99	1.40	2.68	169	236	0.21	1.62	0.73	5.68	6.40
UNSCEAR	33	45	420	[22, 46]	370	≤ 1	≤ 1	≤ 1	≤ 1	≤ 1	59	84	0.07	0.41	0.29	1.16	1.45

Table 12 Activity concentrations and radiological evaluation of incinerated sewage sludge ash (ISSA)

Activity concentration					Radiological evaluation using Eqs. (2–15)												
Material	S (Bq kg^{-1})			References	Ra_{eq} (Bq kg^{-1})	I_γ	I_α	H_{ex}	H_{in}	AUI	AD (nGy h^{-1})		AED (mSv y^{-1})		ELCR ($\times 10^{-3}$)		
	^{226}Ra	^{232}Th	^{40}K								Out	In	Out	In	Out	In	Total
ISSA	65	60	563	[19]	194	0.70	0.33	0.52	0.70	1.37	90	126	0.11	0.90	0.39	3.02	3.41
Average	65	60	563		194	0.70	0.33	0.52	0.70	1.37	90	126	0.11	0.86	0.39	3.02	3.41
UNSCEAR	33	45	420	[22, 46]	370	≤ 1	≤ 1	≤ 1	≤ 1	≤ 1	59	84	0.07	0.41	0.29	1.16	1.45

Table 13 Activity concentrations and radiological evaluation of lead slag (LS)

Activity concentration					Radiological evaluation using Eqs. (2–15)												
Material	S (Bq kg^{-1})			References	Ra_{eq} (Bq kg^{-1})	I_γ	I_α	H_{ex}	H_{in}	AUI	AD (nGy h^{-1})		AED (mSv y^{-1})		ELCR ($\times 10^{-3}$)		
	^{226}Ra	^{232}Th	^{40}K								Out	In	Out	In	Out	In	Total
LS	270	36	200	[73]	337	1.10	1.35	0.91	1.64	2.95	155	217	0.19	1.49	0.67	5.21	5.88
Average	270	36	200		337	1.10	1.35	0.91	1.64	2.95	155	217	0.19	1.49	0.67	5.21	5.88
UNSCEAR	33	45	420	[22, 46]	370	≤ 1	≤ 1	≤ 1	≤ 1	≤ 1	59	84	0.07	0.41	0.29	1.16	1.45

Table 14 Activity concentrations and radiological evaluation of metakaolin (MK)

Activity concentration					Radiological evaluation using Eqs. (2–15)												
Material	S (Bq kg^{-1})			References	Ra_{eq} (Bq kg^{-1})	I_γ	I_α	H_{ex}	H_{in}	AUI	AD (nGy h^{-1})		AED (mSv y^{-1})		ELCR ($\times 10^{-3}$)		
	^{226}Ra	^{232}Th	^{40}K								Out	In	Out	In	Out	In	Total
MK	31	34	188	[76]	94	0.34	0.16	0.25	0.34	0.71	43	60	0.05	0.41	0.18	1.44	1.62
MK	73	63	136	[80]	174	0.60	0.37	0.47	0.67	1.45	77	108	0.10	0.74	0.33	2.61	2.94
MK	125	92	695	[80]	310	1.11	0.63	0.84	1.18	2.32	142	199	0.18	1.37	0.61	4.79	5.40
MK	61	44	590	[102]	169	0.62	0.31	0.46	0.62	1.14	79	111	0.10	0.76	0.34	2.67	3.01
MK	319	272	1,470	[102]	821	2.91	1.60	2.22	3.08	6.35	373	522	0.46	3.59	1.61	12.56	14.16
MK	18	48	31	[103]	89	0.31	0.09	0.24	0.29	0.75	39	54	0.05	0.37	0.17	1.30	1.47
MK	65	99	157	[103]	219	0.76	0.33	0.59	0.77	1.81	96	135	0.12	0.93	0.41	3.24	3.66
MK	82	98	464	[104]	258	0.92	0.41	0.70	0.92	1.98	116	163	0.14	1.12	0.50	3.92	4.42
Average	97	94	466		267	0.95	0.48	0.72	0.98	2.06	121	169	0.15	1.16	0.52	4.07	4.59
UNSCEAR	33	45	420	[22, 46]	370	≤ 1	≤ 1	≤ 1	≤ 1	≤ 1	59	84	0.07	0.41	0.29	1.16	1.45

Table 15 Activity concentrations and radiological evaluation of marble powder (MP)

Activity concentration					Radiological evaluation using Eqs. (2–15)												
Material	S (Bq kg^{-1})			References	Ra_{eq} (Bq kg^{-1})	I_γ	I_α	H_{ex}	H_{in}	AUI	AD (nGy h^{-1})		AED (mSv y^{-1})		ELCR ($\times 10^{-3}$)		
	^{226}Ra	^{232}Th	^{40}K								Out	In	Out	In	Out	In	Total
MP	2	1	10	[80]	4	0.02	0.01	0.01	0.02	0.03	2	3	0.00	0.02	0.01	0.07	0.07
MP	1	3	25	[63]	7	0.03	0.01	0.02	0.02	0.05	3	5	0.00	0.03	0.01	0.11	0.13
MP	1	4	20	[105]	8	0.03	0.01	0.02	0.03	0.06	4	5	0.00	0.04	0.02	0.12	0.14
MP	1	1	4	[106]	3	0.01	0.01	0.01	0.01	0.02	1	2	0.00	0.01	0.01	0.04	0.05
Average	1	2	15		6	0.02	0.01	0.02	0.02	0.04	3	4	0.00	0.02	0.01	0.09	0.10
UNSCEAR	33	45	420	[22, 37]	370	≤ 1	≤ 1	≤ 1	≤ 1	≤ 1	59	84	0.07	0.41	0.29	1.16	1.45

Table 16 Activity concentrations and radiological evaluation of mill tailings (MT)

Activity concentration					Radiological evaluation using Eqs. (2–15)												
Material	S (Bq kg^{-1})			References	Ra_{eq} (Bq kg^{-1})	I_γ	I_α	H_{ex}	H_{in}	AUI	AD (nGy h^{-1})		AED (mSv y^{-1})		ELCR ($\times 10^{-3}$)		
	^{226}Ra	^{232}Th	^{40}K								Out	In	Out	In	Out	In	Total
MT	87	20	226	[107]	133	0.47	0.44	0.36	0.59	1.06	62	86	0.08	0.59	0.27	2.08	2.34
MT	2,668	89	781	[107]	2,855	9.60	13.3	7.72	14.9	25.8	1319	1847	1.62	12.69	5.68	44.40	50.08
MT	650	90	740	[25]	836	2.86	3.25	2.26	4.01	7.15	386	540	0.47	3.71	1.66	12.98	14.64
Average	1,135	66	582		1,275	4.31	5.68	3.44	6.51	11.3	589	824	0.72	5.66	2.53	19.82	22.35
UNSCEAR	33	45	420	[22, 37]	370	≤ 1	≤ 1	≤ 1	≤ 1	≤ 1	59	84	0.07	0.41	0.29	1.16	1.45

2.3 Multivariate item and factor analysis

A Minitab statistical software version 18.1 was used to carry out the multivariate item and factor analysis. Multivariate item and factor analysis is a statistical technique that examine the connections between several variables in an effort to find latent factors that underlie the correlation patterns between those variables. Pearson's correlation matrix was conducted to evaluate the relationship between the strength and direction of the radiological characteristics of agricultural and industrial byproducts. The strength determines the robustness of the relationship, while the direction signifies the coefficient signs

Table 17 Activity concentrations and radiological evaluation of nickel slag (NS)

Activity concentration					Radiological evaluation using Eqs. (2–15)												
Material	S (Bq kg^{-1})			References	Ra_{eq} (Bq kg^{-1})	I_γ	I_α	H_{ex}	H_{in}	AUI	AD (nGy h^{-1})		AED (mSv y^{-1})		ELCR ($\times 10^{-3}$)		
	^{226}Ra	^{232}Th	^{40}K								Out	In	Out	In	Out	In	Total
NS	52	78	76	[73]	169	0.59	0.26	0.46	0.60	1.43	74	104	0.09	0.71	0.32	2.50	2.82
NS	235	45	605	[73]	349	1.21	1.18	0.93	1.57	2.76	161	225	0.20	1.55	0.69	5.42	6.11
Average	143	61	340		258	0.90	0.72	0.70	1.08	2.10	118	165	0.14	1.13	0.51	3.96	4.47
UNSCEAR	33	45	420	[22, 37]	370	≤ 1	≤ 1	≤ 1	≤ 1	≤ 1	59	84	0.07	0.41	0.29	1.16	1.45

Table 18 Activity concentrations and radiological evaluation of pyrite ash (PA)

Activity concentration					Radiological evaluation using Eqs. (2–15)												
Material	S (Bq kg^{-1})			References	Ra_{eq} (Bq kg^{-1})	I_γ	I_α	H_{ex}	H_{in}	AUI	AD (nGy h^{-1})		AED (mSv y^{-1})		ELCR ($\times 10^{-3}$)		
	^{226}Ra	^{232}Th	^{40}K								Out	In	Out	In	Out	In	Total
PA	3	1	16	[80]	6	0.02	0.02	0.02	0.02	0.04	3	4	0.00	0.03	0.01	0.09	0.10
PA	23	16	58	[80]	50	0.18	0.12	0.14	0.20	0.41	23	32	0.03	0.22	0.10	0.76	0.86
Average	12	9	37		28	0.10	0.07	0.08	0.11	0.23	13	18	0.02	0.12	0.05	0.43	0.48
UNSCEAR	33	45	420	[22, 37]	370	≤ 1	≤ 1	≤ 1	≤ 1	≤ 1	59	84	0.07	0.41	0.29	1.16	1.45

Table 19 Activity concentrations and radiological evaluation of phosphogypsum (PG)

Activity concentration					Radiological evaluation using Eqs. (2–15)												
Material	S (Bq kg^{-1})			References	Ra_{eq} (Bq kg^{-1})	I_γ	I_α	H_{ex}	H_{in}	AUI	AD (nGy h^{-1})		AED (mSv y^{-1})		ELCR ($\times 10^{-3}$)		
	^{226}Ra	^{232}Th	^{40}K								Out	In	Out	In	Out	In	Total
PG	491	31	68	[108]	541	1.81	2.46	1.46	2.79	4.92	248	348	0.31	2.39	1.07	8.36	9.43
PG	629	15	10	[80]	651	2.18	3.15	1.76	3.46	5.99	300	420	0.37	2.89	1.29	10.10	11.39
PG	246	50	340	[109]	344	1.18	1.23	0.93	1.59	2.90	158	221	0.19	1.52	0.68	5.32	6.00
PG	234	21	108	[108]	272	0.92	1.17	0.74	1.37	2.42	125	175	0.15	1.21	0.54	4.22	4.76
PG	410	182	34	[110]	673	2.29	2.05	1.82	2.93	5.99	301	421	0.37	2.89	1.29	10.12	11.42
PG	209	17	3	[111]	234	0.78	1.05	0.63	1.20	2.14	107	150	0.13	1.03	0.46	3.60	4.06
PG	115	31	95	[111]	167	0.57	0.58	0.45	0.76	1.44	76	106	0.09	0.73	0.33	2.55	2.88
PG	322	18	116	[108]	357	1.20	1.61	0.96	1.83	3.20	164	230	0.20	1.58	0.71	5.54	6.24
PG	306	23	17	[111]	340	1.14	1.53	0.92	1.75	3.11	156	218	0.19	1.50	0.67	5.25	5.92
PG	305	20	110	[111]	342	1.15	1.53	0.92	1.75	3.07	158	221	0.19	1.52	0.68	5.30	5.98
PG	440	12	235	[111]	475	1.61	2.20	1.28	2.47	4.23	220	308	0.27	2.12	0.95	7.42	8.37
PG	233	30	323	[109]	301	1.03	1.17	0.81	1.44	2.54	139	195	0.17	1.34	0.60	4.69	5.29
PG	747	14	63	[108]	772	2.58	3.74	2.09	4.10	7.08	356	499	0.44	3.43	1.53	11.99	13.52
PG	378	4	40	[108]	387	1.29	1.89	1.05	2.07	3.54	179	250	0.22	1.72	0.77	6.02	6.79
PG	618	9	24	[108]	633	2.11	3.09	1.71	3.38	5.82	292	409	0.36	2.81	1.26	9.83	11.08
PG	340	4	200	[112]	361	1.22	1.70	0.98	1.89	3.21	168	235	0.21	1.61	0.72	5.65	6.37
PG	35	72	585	[109]	183	0.67	0.18	0.49	0.59	1.24	84	118	0.10	0.81	0.36	2.83	3.19
PG	750	1	14	[113]	753	2.51	3.75	2.03	4.06	6.94	348	487	0.43	3.34	1.50	11.70	13.20
Average	378	31	133		432	1.46	1.89	1.17	2.19	3.88	199	278	0.24	1.91	0.86	6.69	7.55
UNSCEAR	33	45	420	[22, 37]	370	≤ 1	≤ 1	≤ 1	≤ 1	≤ 1	59	84	0.07	0.41	0.29	1.16	1.45

Table 20 Activity concentrations and radiological evaluation of pumice (PM)

Activity concentration					Radiological evaluation using Eqs. (2–15)												
Material	S (Bq kg^{-1})			References	Ra_{eq} (Bq kg^{-1})	I_γ	I_α	H_{ex}	H_{in}	AUI	AD (nGy h^{-1})		AED (mSv y^{-1})		ELCR ($\times 10^{-3}$)		
	^{226}Ra	^{232}Th	^{40}K								Out	In	Out	In	Out	In	Total
PM	12	12	300	[80]	52	0.20	0.06	0.14	0.17	0.28	25	35	0.03	0.24	0.11	0.85	0.96
PM	24	21	653	[80]	104	0.40	0.12	0.28	0.35	0.53	51	71	0.06	0.49	0.22	1.72	1.94
PM	75	74	1,073	[17]	263	0.98	0.38	0.71	0.91	1.67	124	174	0.15	1.19	0.53	4.18	4.71
PM	462	57	1	[17]	544	1.83	2.31	1.47	2.72	4.96	248	347	0.30	2.38	1.07	8.35	9.41
Average	143	41	507		241	0.85	0.72	0.65	1.04	1.86	112	157	0.14	1.08	0.48	3.77	4.26
UNSCEAR	33	45	420	[22, 46]	370	≤ 1	≤ 1	≤ 1	≤ 1	≤ 1	59	84	0.07	0.41	0.29	1.16	1.45

Table 21 Activity concentrations and radiological evaluation of red mud/bauxite powder (RM)

Activity concentration					Radiological evaluation using Eqs. (2–15)												
Material	S (Bq kg^{-1})			References	Ra_{eq} (Bq kg^{-1})	I_γ	I_α	H_{ex}	H_{in}	AUI	AD (nGy h^{-1})		AED (mSv y^{-1})		ELCR ($\times 10^{-3}$)		
	^{226}Ra	^{232}Th	^{40}K								Out	In	Out	In	Out	In	Total
RM	310	1,350	350	[85]	2,267	7.90	1.55	6.12	6.96	19.2	973	1363	1.20	9.36	4.19	32.76	36.95
RM	139	350	45	[73]	643	2.23	0.70	1.74	2.11	5.52	277	388	0.34	2.67	1.19	9.34	10.54
RM	380	507	361	[85]	1,133	3.92	1.90	3.06	4.09	9.67	497	696	0.61	4.78	2.14	16.73	18.86
RM	306	408	33	[114]	892	3.07	1.53	2.41	3.24	7.76	389	545	0.48	3.74	1.68	13.10	14.78
RM	289	285	121	[85]	706	2.43	1.45	1.91	2.69	6.12	311	435	0.38	2.99	1.34	10.46	11.80
RM	97	118	15	[73]	267	0.92	0.49	0.72	0.98	2.32	117	163	0.14	1.12	0.50	3.93	4.43
RM	710	339	300	[73]	1,218	4.16	3.55	3.29	5.21	10.7	545	763	0.67	5.24	2.35	18.36	20.70
RM	210	539	112	[73]	989	3.43	1.05	2.67	3.24	8.46	427	598	0.53	4.11	1.84	14.38	16.22
RM	165	328	53	[85]	638	2.21	0.83	1.72	2.17	5.49	277	387	0.34	2.66	1.19	9.31	10.50
RM	347	283	48	[85]	755	2.59	1.74	2.04	2.98	6.63	333	467	0.41	3.21	1.43	11.22	12.65
RM	370	328	265	[85]	859	2.96	1.85	2.32	3.32	7.40	380	532	0.47	3.66	1.64	12.80	14.43
RM	232	344	45	[85]	727	2.51	1.16	1.96	2.59	6.30	317	444	0.39	3.05	1.36	10.67	12.03
RM	379	472	21	[85]	1,056	3.63	1.90	2.85	3.88	9.21	461	645	0.57	4.43	1.98	15.52	17.51
RM	370	437	505	[85]	1,034	3.59	1.85	2.79	3.79	8.74	456	638	0.56	4.39	1.96	15.35	17.31
RM	350	414	583	[85]	987	3.43	1.75	2.67	3.61	8.28	436	610	0.54	4.19	1.88	14.68	16.56
RM	478	555	401	[85]	1,303	4.50	2.39	3.52	4.81	11.2	573	802	0.70	5.51	2.47	19.28	21.75
RM	255	422	164	[85]	871	3.01	1.28	2.35	3.04	7.47	380	531	0.47	3.65	1.63	12.78	14.41
RM	477	705	153	[85]	1,497	5.17	2.39	4.04	5.33	12.9	653	914	0.80	6.28	2.81	21.97	24.78
RM	326	1,129	30	[85]	1,943	6.74	1.63	5.25	6.13	16.7	834	1167	1.03	8.02	3.59	28.07	31.66
RM	318	1,320	190	[85]	2,220	7.72	1.59	6.00	6.85	18.9	952	1333	1.17	9.16	4.10	32.05	36.15
RM	17	63	625	[91]	155	0.58	0.09	0.42	0.47	0.97	72	101	0.09	0.69	0.31	2.42	2.73
RM	100	113	55	[76]	266	0.92	0.50	0.72	0.99	2.29	117	163	0.14	1.12	0.50	3.93	4.43
RM	97	118	50	[17]	270	0.93	0.49	0.73	0.99	2.33	118	165	0.15	1.14	0.51	3.98	4.49
RM	301	539	215	[17]	1,088	3.77	1.51	2.94	3.75	9.31	474	663	0.58	4.55	2.04	15.94	17.98
RM	170	404	26	[2]	750	2.60	0.85	2.02	2.48	6.45	324	453	0.40	3.11	1.39	10.89	12.29
RM	203	598	62	[115]	1,063	3.69	1.02	2.87	3.42	9.10	458	641	0.56	4.40	1.97	15.40	17.37
RM	225	219	5	[116]	539	1.85	1.13	1.45	2.06	4.72	236	331	0.29	2.27	1.02	7.96	8.98
RM	568	392	101	[116]	1,136	3.89	2.84	3.07	4.60	9.99	503	705	0.62	4.84	2.17	16.95	19.11
Average	292	467	176		974	3.37	1.46	2.63	3.42	8.36	425	594	0.52	4.08	1.83	14.29	16.12
UNSCEAR	33	45	420	[22, 46]	370	≤ 1	≤ 1	≤ 1	≤ 1	≤ 1	59	84	0.07	0.41	0.29	1.16	1.45

Table 22 Activity concentrations and radiological evaluation of silica fume (SF)

Activity concentration					Radiological evaluation using Eqs. (2–15)												
Material	S (Bq kg^{-1})			References	Ra_{eq} (Bq kg^{-1})	I_γ	I_α	H_{ex}	H_{in}	AUI	AD (nGy h^{-1})		AED (mSv y^{-1})		ELCR ($\times 10^{-3}$)		
	^{226}Ra	^{232}Th	^{40}K								Out	In	Out	In	Out	In	Total
SF	2	3	100	[92]	14	0.06	0.01	0.04	0.04	0.06	7	10	0.01	0.07	0.03	0.23	0.26
SF	1	2	92	[92]	11	0.04	0.01	0.03	0.03	0.04	6	8	0.01	0.05	0.02	0.19	0.21
SF	1	0	870	[82]	68	0.29	0.01	0.18	0.19	0.08	37	51	0.05	0.35	0.16	1.24	1.39
SF	33	24	540	[62]	109	0.41	0.17	0.29	0.38	0.64	52	73	0.06	0.50	0.22	1.76	1.98
SF	4	6	297	[117]	35	0.14	0.02	0.10	0.11	0.13	18	25	0.02	0.17	0.08	0.60	0.68
SF	0	0	100	[76]	8	0.03	0.00	0.02	0.02	0.01	4	6	0.01	0.04	0.02	0.14	0.16
SF	0	0	92	[76]	7	0.03	0.00	0.02	0.02	0.01	4	5	0.00	0.04	0.02	0.13	0.15
Average	6	5	299		36	0.14	0.03	0.10	0.11	0.14	18	25	0.02	0.17	0.08	0.61	0.69
UNSCEAR	33	45	420	[22, 46]	370	≤ 1	≤ 1	≤ 1	≤ 1	≤ 1	59	84	0.07	0.41	0.29	1.16	1.45

Table 23 Activity concentrations and radiological evaluation of steel slag (SS)

Activity concentration					Radiological evaluation using Eqs. (2–15)												
Material	S (Bq kg^{-1})			References	Ra_{eq} (Bq kg^{-1})	I_γ	I_α	H_{ex}	H_{in}	AUI	AD (nGy h^{-1})		AED (mSv y^{-1})		ELCR ($\times 10^{-3}$)		
	^{226}Ra	^{232}Th	^{40}K								Out	In	Out	In	Out	In	Total
SS	5	0	1	[71]	5	0.02	0.03	0.01	0.03	0.05	2	3	0.00	0.02	0.01	0.08	0.09
SS	23	21	0	[76]	53	0.18	0.12	0.14	0.21	0.47	23	33	0.03	0.22	0.10	0.78	0.89
SS	23	15	4	[76]	45	0.15	0.12	0.12	0.18	0.39	20	28	0.02	0.19	0.09	0.67	0.75
SS	16	20	0	[76]	45	0.15	0.08	0.12	0.16	0.39	19	27	0.02	0.19	0.08	0.66	0.74
SS	20	16	0	[76]	43	0.15	0.10	0.12	0.17	0.38	19	26	0.02	0.18	0.08	0.64	0.72
SS	62	21	51	[73]	96	0.33	0.31	0.26	0.43	0.83	43	61	0.05	0.42	0.19	1.46	1.65
SS	23	15	51	[73]	48	0.17	0.12	0.13	0.19	0.40	22	31	0.03	0.21	0.09	0.73	0.83
SS	13	7	21	[73]	25	0.09	0.07	0.07	0.10	0.21	11	16	0.01	0.11	0.05	0.37	0.42
SS	25	5	10	[73]	33	0.11	0.13	0.09	0.16	0.29	15	21	0.02	0.14	0.06	0.50	0.57
SS	196	30	148	[73]	250	0.85	0.98	0.68	1.21	2.19	115	161	0.14	1.10	0.49	3.87	4.36
SS	0	150	0	[73]	215	0.75	0.00	0.58	0.58	1.81	91	127	0.11	0.87	0.39	3.05	3.44
SS	88	49	0	[73]	158	0.54	0.44	0.43	0.66	1.41	70	98	0.09	0.68	0.30	2.36	2.67
Average	41	29	24		85	0.29	0.21	0.23	0.34	0.73	38	53	0.05	0.36	0.16	1.27	1.43
UNSCEAR	33	45	420	[22, 46]	370	≤ 1	≤ 1	≤ 1	≤ 1	≤ 1	59	84	0.07	0.41	0.29	1.16	1.45

Table 24 Activity concentrations and radiological evaluation of tin slag (TS)

Activity concentration					Radiological evaluation using Eqs. (2–15)												
Material	S (Bq kg^{-1})			References	Ra_{eq} (Bq kg^{-1})	I_γ	I_α	H_{ex}	H_{in}	AUI	AD (nGy h^{-1})		AED (mSv y^{-1})		ELCR ($\times 10^{-3}$)		
	^{226}Ra	^{232}Th	^{40}K								Out	In	Out	In	Out	In	Total
TS	1,100	300	330	[73]	1,554	5.3	5.50	4.2	7.2	13.8	703	984	0.9	6.8	3.0	23.7	26.7
TS	6,428	420	0	[73]	7,029	23.5	32.1	19.0	36.4	64.5	3223	4513	4.0	31.0	13.9	108.5	122.4
TS	1,000	4,000	0	[73]	6,720	23.3	5.00	18.1	20.8	57.6	2878	4029	3.5	27.7	12.4	96.9	109.3
Average	2,843	1,573	110		5,101	17.4	14.2	13.8	21.5	45.3	2268	3175	2.8	21.8	9.8	76.4	86.1
UNSCEAR	33	45	420	[22, 46]	370	≤ 1	≤ 1	≤ 1	≤ 1	≤ 1	59	84	0.07	0.41	0.29	1.16	1.45

Table 25 Activity concentrations and radiological evaluation of volcanic ash (VA)

Activity concentration					Radiological evaluation using Eqs. (2–15)												
Material	S (Bq kg^{-1})			References	Ra_{eq} (Bq kg^{-1})	I_γ	I_α	H_{ex}	H_{in}	AUI	AD (nGy h^{-1})		AED (mSv y^{-1})		ELCR ($\times 10^{-3}$)		
	^{226}Ra	^{232}Th	^{40}K								Out	In	Out	In	Out	In	Total
VA	59	132	1,130	[80]	335	1.23	0.30	0.90	1.06	2.23	154	216	0.19	1.48	0.66	5.19	5.85
VA	92	138	1,200	[105]	382	1.40	0.46	1.03	1.28	2.62	176	246	0.22	1.69	0.76	5.92	6.68
VA	190	210	1,900	[105]	637	2.32	0.95	1.72	2.23	4.45	294	411	0.36	2.83	1.27	9.89	11.2
VA	280	270	1,900	[105]	812	2.92	1.40	2.19	2.95	6.00	372	520	0.46	3.57	1.60	12.5	14.1
Average	155	188	1,533		541	1.97	0.78	1.46	1.88	3.83	249	348	0.31	2.39	1.07	8.38	9.45
UNSCEAR	33	45	420	[22, 46]	370	≤ 1	≤ 1	≤ 1	≤ 1	≤ 1	59	84	0.07	0.41	0.29	1.16	1.45

Table 26 Activity concentrations and radiological evaluation of waste glass powder (WP)

Activity concentration					Radiological evaluation using Eqs. (2–15)s												
Material	S (Bq kg^{-1})			References	Ra_{eq} (Bq kg^{-1})	I_γ	I_α	H_{ex}	H_{in}	AUI	AD (nGy h^{-1})		AED (mSv y^{-1})		ELCR ($\times 10^{-3}$)		
	^{226}Ra	^{232}Th	^{40}K								Out	In	Out	In	Out	In	Total
WP	8	11	227	[92]	41	0.16	0.04	0.11	0.13	0.23	20	28	0.02	0.19	0.09	0.67	0.75
WP	9	11	2	[76]	25	0.09	0.05	0.07	0.09	0.22	11	15	0.01	0.10	0.05	0.37	0.41
Average	9	11	115		33	0.12	0.04	0.09	0.11	0.22	15	21	0.02	0.15	0.07	0.52	0.58
UNSCEAR	33	45	420	[22, 46]	370	≤ 1	≤ 1	≤ 1	≤ 1	≤ 1	59	84	0.07	0.41	0.29	1.16	1.45

of the relationship. The correlation coefficients range in value from −1 to + 1. The reliability index (internal consistency) was statistically analyzed via Cronbach's alpha to assess how the radiological parameters reliably measure the same construct or characteristics. A Cronbach's alpha with a low value may not reliably measure a single construct. Typically, a value of 0.7 or higher is considered good [50]. Multivariate factor analysis was also engaged in evaluating the data correlation among variables in terms of a few underlying unobservable random factors of the radiological data (16 variables). In factor analysis, the original variables are expressed as linear combinations of the factors. Principal components were used as an extraction method, while the rotated factor analysis was conducted by varimax. Varimax is the most widely used rotation method [41]. This method makes the loadings either large or small for an easy explanation.

3 Results and discussion

3.1 Agricultural byproducts

The results of radiological properties of agricultural byproducts are presented in Tables 2, 3, 4, 5. The results showed that the ^{226}Ra, ^{232}Th, and ^{40}K of all studied byproducts varied between 1–14.1 Bq kg^{-1}, 1.3–16 Bq kg^{-1}, and 81.4–604 Bq kg^{-1} with average values of 6, 16, and 5055 Bq kg^{-1} for RHA in Table 2, 7.99, 5.08, and 175 Bq kg^{-1} for MS in Table 3, 6.41, 4.56, and 584 Bq kg^{-1} for POC in Table 4, and 8.10, 7.02, and 477 Bq kg^{-1} for POFA in Table 5. The ^{226}Ra, ^{232}Th, and ^{40}K activities were in the range of the UNSCEAR values of 33, 45, and 420 Bq kg^{-1} [22, 46], except for the RHA, POC, and POFA, whose ^{40}K were about 17, 28, and 6% higher than the world population weighted average values. Geographical, geochemical, and geological variations in the soil composition from which rice and palm oil plants absorb radionuclides might be the causes of the variations in the activity concentrations of the RHA, POC, and POFA samples. Materials origins and radioactive mineral content are also factors [24, 51]. During the burning process, various chemical and physical changes would occur, including eliminating organic components and moisture found in nuts, fiber, rice shells, and palm oil. Thus, these radionuclides are enriched or redistributed in RHA, POC, and POFA [52]. The ^{40}K isotopes in RHA, POC, and POFA satisfied the world range of 140–850 Bq kg^{-1} proposed for building materials [46]. The ^{226}Ra, ^{232}Th, and ^{40}K of the studied byproducts (RHA, MS, POC, POFA) also met the internationally

recognized weighted average values of 50, 50, and 500 Bq kg^{-1} [11, 53], as well as the ranges of 100–600, 30–300, and 100–1,200 Bq kg^{-1} proposed for ^{226}Ra, ^{232}Th, and ^{40}K isotopes [12].

As depicted in Tables 2, 3, 4, 5, the results of Ra_{eq} activities for all studied byproducts were less than the upper mean limit of 370 Bq kg^{-1} for building materials to keep the external dose below 1.5 mSv y^{-1} [11]. The Ra_{eq} values varied between 18 and 68 Bq kg^{-1} with the averages of 68, 29, 58, and 53 Bq kg^{-1} for RHA, MS, POC, and POFA in Tables 2, 3, 4, 5. The Ra_{eq} is associated with the activity concentration, hazard, and activity utilization indexes due to radon and its daughter [54]. For safe use, the maximum value for gamma and alpha indexes, external and internal hazard indexes, and utilization concentration correspond to 370 Bq kg^{-1} upper limit of Ra_{eq}. Owing to this fact, the values obtained for I_γ, I_α, H_{ex}, H_{in}, and AUI are low because they are derived from the low activity concentrations of ^{226}Ra, ^{232}Th, and ^{40}K. Compared with the global recommendation, all indexes obtained for the studied agricultural byproducts were below the 1.0 maximum [22, 46]. The low emission factor by the radon's alpha recoil range in materials can be attributable to the low values, roughly a few tens of nanometers [55].

The results of RHA, MS, POC, and POFA, as shown in Tables 2, 3, 4, 5, revealed that the AD_{out} and AD_{in} rates varied between 9–33 nGy h^{-1} and 13–47 nGy h^{-1}, corresponding to the average values of 20 and 27 nGy h^{-1}. The AED_{out} and AED_{in} rates varied between 0.011–0.041 mSv y^{-1} and 0.10–0.31 mSv y^{-1}, corresponding to the average values of 0.02 and 0.18 mSv y^{-1}. The obtained results were less than the globally recognized limits reported by UNSCEAR [22, 46], which are 59 nGy h^{-1} for AD_{out}, 84 nGy h^{-1} for AD_{in}, 0.07 mSv y^{-1} for AED_{out}, and 0.41 mSv y^{-1} for AED_{in}. The average calculated values of excess lifetime cancer risks, as presented in Tables 6, 7, 8, 9, 10, 11, 12, 13, 14, 15, 16, 17, 18, 19, 20, 21, 22, 23, 24, 25, and 26, were 0.11×10^{-3} for outdoors, 0.88×10^{-3} for indoors, and 0.99×10^{-3} for total. By comparison, these results were less than the world population-weighted average values [22, 46], which are 0.29×10^{-3} for outdoors, 1.16×10^{-3} for indoors, and 1.45×10^{-3} for total ELCR. Strictly speaking, no results shown in Tables 2, 3, 4, 5 should be equally treated. This is due to the possibility of using various techniques, such as instruments, and varying the circumstances around the samples and their surroundings when making the measurements [55]. According to the literature, the radiological performances of materials are influenced by the instruments' characteristics and environmental factors [55].

The earth-originated materials are primarily used in the construction of buildings, making the concentrations of all indoor exposures, as shown in Tables 2, 3, 4, 5, higher than the outdoor exposures. Besides, agricultural byproducts are soil-originated materials, exhibiting ^{40}K rather than ^{226}Ra and ^{232}Th (Tables 2, 3, 4, 5) [22]. From all indications and indices, the considered radioactive parameters from naturally occurring radioactive contents in RHA, MS, POC, and POFA are permissible to the global recommendation levels, satisfying the world population-weighted average values [22, 46]. RHA, MS, POC, and POFA pose no potential radiological risk and can be safely used as building and construction materials.

3.2 Industrial byproducts

Unlike agricultural byproducts, the radiological properties of recycled industrial waste materials, as shown in Tables 6, 7, 8, 9, 10, 11, 12, 13, 14, 15, 16, 17, 18, 19, 20, 21, 22, 23, 24, 25, and 26, exhibited higher activity concentrations than the proposed values of UNSCEAR, except for marble powder (MP), pyrite ash (PA), silica fume (SF), steel slag (SS), and waste glass powder (WP) in Tables 15, 18, 22, 23, and 26. The average activity concentrations of ^{226}Ra and ^{232}Th (Tables 6 and 8) were about 83.18–101.13% and 13.46–40.79% higher than the world average values for BA and CS. The ^{226}Ra and ^{232}Th for BM (Table 3) were below the average world value proposed by UNSCEAR [22, 46]. The ^{40}K was about 99% and 43% higher than the world average values for BM and CS, resulting in an effective annual dose above 1 mSv y^{-1}. The ^{40}K in BA (Table 6) was about 17% less. Except for the ^{40}K of GGBFS in Table 10, which was almost 42% below the population-weighted global average value, all activity concentrations for FA and GGBFS in Tables 9, 10 exceeded the global average limits. The average activity concentrations of GWP, ISSA, LS, and MK in Tables 11, 12, 13, 14 were 2–4, 1–2, 8, and 1–2 times more than the world average limits. In contrast, the ^{232}Th and ^{40}K of LS in Table 13 were 1–2 times below the world's average recommendation. Regarding MT, NS, and PG in Tables 16, 17, and 19, the average values for ^{226}Ra were 34, 4, and 11 times higher than the average world value. The corresponding average values (^{232}Th and ^{40}K) for NS and PG were 1–3 times less than the world average stipulations.

As shown in Tables 15 and 18, the average activity concentrations for MP and PA were 15–33 and 3–12 times less than the UNSCEAR values. The ^{226}Ra, ^{232}Th, and ^{40}K average activities obtained for PM and RM in Tables 20 and 21 exceeded the world average values by 1–4 and 9–10 times. Nonetheless, the ^{232}Th of PM and ^{40}K of RM were less than the world average values. It is apparent from Tables 22, 23, and 26 that the average activity concentrations for SF, SS, and WP were

Table 27 Pearson correlation coefficients of agricultural byproducts (RHA, MS, POC, and POFA), Cronbach's alpha = 0.9657

Variable	^{226}Ra	^{232}Th	^{40}K	Ra_{eq}	I_{γ}	I_{α}	H_{ex}	H_{in}	AUI	AD_{out}	AD_{in}	AED_{out}	AED_{in}	$ECLR_{out}$	$ECLR_{in}$	$ECLR_{total}$
^{226}Ra	1.000															
^{232}Th	0.358	1.000														
^{40}K	−0.309	0.140	1.000													
Ra_{eq}	−0.026	0.455	0.933	1.000												
Iγ	−0.068	0.400	0.952	0.996	1.000											
Iα	0.980	0.382	−0.301	−0.015	−0.061	1.000										
H_{ex}	−0.024	0.448	0.917	0.985	0.981	−0.034	1.000									
H_{in}	0.049	0.434	0.828	0.909	0.898	0.037	0.921	1.000								
AUI	0.652	0.889	0.241	0.574	0.520	0.664	0.561	0.568	1.000							
AD_{out}	−0.066	0.395	0.953	0.997	0.997	−0.054	0.981	0.906	0.521	1.000						
AD_{in}	−0.072	0.406	0.953	0.998	0.998	−0.062	0.982	0.904	0.524	0.999	1.000					
AED_{out}	−0.068	0.390	0.955	0.997	0.999	−0.059	0.980	0.901	0.517	0.999	0.999	1.000				
AED_{in}	−0.025	0.498	0.850	0.935	0.912	−0.001	0.926	0.849	0.582	0.930	0.931	0.920	1.000			
$ECLR_{out}$	−0.076	0.371	0.957	0.992	0.994	−0.068	0.972	0.901	0.502	0.996	0.996	0.997	0.911	1.000		
$ECLR_{in}$	−0.072	0.396	0.955	0.997	0.998	−0.062	0.982	0.903	0.518	0.999	1.000	1.000	0.927	0.997	1.000	
$ECLR_{total}$	−0.071	0.393	0.955	0.997	0.999	−0.061	0.981	0.901	0.517	0.999	1.000	1.000	0.926	0.997	1.000	1.000

Table 28 Pearson correlation coefficients of industrial byproducts within the permissible limits of world population-weighted average values, Cronbach's alpha = 0.9842

Variable	^{226}Ra	^{232}Th	^{40}K	Ra_{eq}	I_{γ}	I_{α}	H_{ex}	H_{in}	AUI	AD_{out}	AD_{in}	AED_{out}	AED_{in}	$ECLR_{out}$	$ECLR_{in}$	$ECLR_{total}$
^{226}Ra	1.000															
^{232}Th	0.183	1.000														
^{40}K	−0.008	−0.125	1.000													
Ra_{eq}	0.753	0.743	0.148	1.000												
Iγ	0.731	0.739	0.206	0.998	1.000											
Iα	1.000	0.183	−0.008	0.753	0.753	1.000										
H_{ex}	0.753	0.743	0.148	1.000	0.998	0.753	1.000									
H_{in}	0.904	0.559	0.093	0.962	0.952	0.904	0.962	1.000								
AUI	0.785	0.752	−0.056	0.978	0.964	0.785	0.978	0.962	1.000							
AD_{out}	0.768	0.705	0.202	0.998	0.998	0.768	0.998	0.967	0.521	1.000						
AD_{in}	0.768	0.705	0.202	0.998	0.998	0.768	0.998	0.967	0.524	0.966	1.000					
AED_{out}	0.768	0.705	0.202	0.998	0.998	0.768	0.998	0.967	0.517	0.966	1.000	1.000				
AED_{in}	0.768	0.705	0.202	0.998	0.998	0.768	0.998	0.967	0.582	0.966	1.000	1.000	1.000			
$ECLR_{out}$	0.768	0.705	0.202	0.998	0.998	0.768	0.998	0.967	0.502	0.966	1.000	1.000	1.000	1.000		
$ECLR_{in}$	0.768	0.705	0.202	0.998	0.998	0.768	0.998	0.967	0.518	0.966	1.000	1.000	1.000	1.000	1.000	
$ECLR_{total}$	0.768	0.705	0.202	0.998	0.998	0.768	0.998	0.967	0.517	0.966	1.000	1.000	1.000	1.000	1.000	1.000

1–9, 1–21, and 3–4 times less than the UNSCEAR values. As displayed in Tables 24 and 25, the activity concentrations of TS and VA were 35–86 and 4–5 times more than the UNSCEAR recommendations.

Some factors are known to influence the low rate (MP, PA, SF, SS, and WP) and high rate (BA, BM, CS, FA, GGBFS, GWP, ISSA, LS, MK, MT, NS, PG, TS, and VA) of activity concentrations in industrial byproducts. Industrial byproducts tend to be more radioactive than agricultural byproducts due to the nature of the materials and processes involved in industrial activities. Many industrial byproducts, such as BM and FA, can contain higher levels of naturally occurring radioactive elements or are produced from processes that involve radioactive substances. For instance, recycling materials leads to the concentration of radioactive isotopes, less commonly a factor in agriculture-related byproducts primarily from biological processes. Agricultural byproducts usually do not interact with radioactive materials directly, whereas industrial byproducts can be influenced by the mining, processing, and use of radioactive minerals. Kovler [14], Sas

Table 29 Pearson correlation coefficients of industrial byproducts above the permissible limits of world population-weighted average values, Cronbach's alpha = 0.9841

Variable	^{226}Ra	^{232}Th	^{40}K	Ra_{eq}	I_γ	I_α	H_{ex}	H_{in}	AUI	AD_{out}	AD_{in}	AED_{out}	AED_{in}	$ECLR_{out}$	$ECLR_{in}$	$ECLR_{total}$
^{226}Ra	1.000															
^{232}Th	0.170	1.000														
^{40}K	−0.059	−0.059	1.000													
Ra_{eq}	0.741	0.692	0.275	1.000												
Iγ	0.702	0.679	0.359	0.996	1.000											
Iα	1.000	0.170	−0.059	0.741	0.702	1.000										
H_{ex}	0.741	0.692	0.275	1.000	0.996	0.741	1.000									
H_{in}	0.902	0.518	0.152	0.958	0.939	0.902	0.958	1.000								
AUI	0.811	0.713	−0.034	0.951	0.919	0.811	0.951	0.957	1.000							
AD_{out}	0.740	0.647	0.344	0.997	0.998	0.740	0.997	0.956	0.927	1.000						
AD_{in}	0.740	0.647	0.344	0.997	0.998	0.740	0.997	0.956	0.927	1.000	1.000					
AED_{out}	0.740	0.647	0.344	0.997	0.998	0.740	0.997	0.956	0.927	1.000	1.000	1.000				
AED_{in}	0.740	0.647	0.344	0.997	0.998	0.740	0.997	0.956	0.927	1.000	1.000	1.000	1.000			
$ECLR_{out}$	0.740	0.647	0.344	0.997	0.998	0.740	0.997	0.956	0.927	1.000	1.000	1.000	1.000	1.000		
$ECLR_{in}$	0.740	0.647	0.344	0.997	0.998	0.740	0.997	0.956	0.927	1.000	1.000	1.000	1.000	1.000	1.000	
$ECLR_{total}$	0.740	0.647	0.344	0.997	0.998	0.740	0.997	0.956	0.927	1.000	1.000	1.000	1.000	1.000	1.000	1.000

et al. [19], and Walencik-Lata and Smolka-Danielowska [58] pointed out that the mechanism of comparing various raw materials is ambiguous because the origin, treatment, processing, and production patterns of raw materials are distinct. PG originating from phosphate rocks possesses higher concentrations of ^{226}Ra than gypsum from carbonate rocks because the phosphate rocks are typically characterized by higher natural radioactivity [14, 17]. This is evident in Table 10, where PG exhibited higher ^{226}Ra, lesser ^{232}Th, and ^{40}K than the world population-weighted average values. The activity concentrations of FA and GGBFS depend on the ore type, origin, and metallurgical processes [14, 59]. During the production processes, several chemical and physical changes, such as removing organic components and moisture from ash and slags, would occur, resulting in the enrichment/redistribution of activity concentration of ^{226}Ra, ^{232}Th, and ^{40}K. Previous studies have established that the utilization of GWP, RM, VA, BM, BA, MT, MK, and PM increased the activity concentrations of the mixtures [25, 60].

The radium equivalent activity (Ra_{eq}), a weighted sum of the activity concentrations of ^{226}Ra, ^{232}Th, and ^{40}K, was also analyzed, and the results are presented in Tables 6, 7, 8, 9, 10, 11, 12, 13, 14, 15, 16, 17, 18, 19, 20, 21, 22, 23, 24, 25, and 26. As explained earlier, a radioactive-safe utilization of byproducts requires a maximum Ra_{eq} of 370 Bq kg^{-1} to maintain an effective dose at 1.0 mSv y^{-1} maximum [7, 22]. From Tables 6, 7, 8, 9, 10, 11, 12, 13, 14, 15, 16, 17, 18, 19, 20, 21, 22, 23, 24, 25, and 26, it is apparent that only eight industrial byproducts (BM, CS, FA, MT, PG, RM, TS, and VA) yielded a higher Ra_{eq} than the UNSCEAR value of 370 Bq kg^{-1}. The other industrial byproducts (BA, GGBFS, GWP, ISSA, LS, MK, MP, NS, PA, PM, SF, SS, and WP) were within the proposed limit. As provided in Tables 7 and 8, the average Ra_{eq} of BM and CS were 45.41 and 114.32% higher, while that of BA in Table 6 was 5.34% less than the average world value of 370 Bq kg^{-1}. The average Ra_{eq} of 30 samples for FA in Table 9 exceeded the world average stipulation by 14%; GGBFS in Table 10 was 28.38% lesser. GWP, ISSA, LS, and MK, as provided in Tables 11, 12, 13, and 14, were below the average world Ra_{eq} by 1.35, 47.57, 8.92, and 27.84%. The average values of MP, NS, and PA in Tables 15, 17, and 18 were 98.38, 30.27, and 92.43% less than the average world Ra_{eq} of 370 Bq kg^{-1}, but MT and PG in Table 16 and 19 were 244.60 and 16.76% higher. The average Ra_{eq} of PM in Table 20 was reduced by 34.87% compared to the UNSCEAR value. RM in Table 21 was exceeded by 163.2 4%. Tables 22, 23, and 26 exhibited a 90.27, 77.03, and 91.08% reduction in the average Ra_{eq} for SF, SS, and WP compared to the UNSCEAR value of 370 Bq kg^{-1}. TS and VA in Tables 24 and 25 surpassed the UNSCEAR value by 1278.65 and 46.22%.

From the radiological viewpoint, evaluating the materials' suitability is crucial. The index analyses were carried out on the surveyed industrial byproducts, and the results are provided in Tables 6, 7, 8, 9, 10, 11, 12, 13, 14, 15, 16, 17, 18, 19, 20, 21, 22, 23, 24, 25, and 26. The results revealed that all indexes (I_γ, I_α, H_{ex}, H_{in}, and AUI) for MP, PA, SF, SS, and WP in Tables 15, 18, 22, 23, and 26 were within the world population-weighted average value of unity (1) recommended by EC (2014) and UNSCEAR [22, 46]. A value of unity, except for H_{in} and AUI, was obtained for FA, GGBFS, NS, and PM in Tables 9,

10, 17, and 20. Tables 12 and14 show that all indexes for ISSA and MK were within the UNSCEAR value of 1, except for AUI, which was greater than unity. All indexes obtained for BA, BM, CS, GWP and LS (except for I_γ and H_{ex}), MT, PG, RM, TS, and VA (except for I_α) in Tables 6, 7, 8, 11 and 13, 16, 19, 21, 24, and 25 were beyond the average world value of 1. It should be noted that index parameters are derived from activity concentrations; these results are consistent with recent research that shows that a material's radium equivalent activity, activity concentration indexes, hazard indexes, and activity utilization indexes increase as activity concentration increases [61]. The radioactive indexes of GGBFS, FA, RM, and PG were approximately 2–8 times more than the UNSCEAR values [62] because of their higher activity concentrations.

Tables 6, 7, 8, 9, 10, 11, 12, 13, 14, 15, 16, 17, 18, 19, 20, 21, 22, 23, 24, 25, and 26 also provide the results of absorbed gamma dose rates (AD) of surveyed industrial byproducts. Tables 6, 7, 8 show that BA, BM, and CS were about 3, 19, and 7 times higher than the UNSCEAR values of 54 and 89 nGy h^{-1} for AD_{out} and AD_{in} rates. From Tables 9, 10, 11, 12, 13, 14, FA, GGBFS, GWP, ISSA, LS, and MK were approximately 2–3 times higher than the world average values. The AD results of NS, PG, PM, RM, and VA in Tables 17, 19, 20, 21, and 25 were about 2–4 times higher; MT and TS in Tables 16 and 24 were approximately 10 and 39 times more than the world average values. As shown in Tables 15, 19, 23, 24, and 26 for MP, PA, SF, SS, and WP, the results revealed that AD_{out} and AD_{in} were about 21, 5, 4, 2, and 4 times less than the UNSCEAR values. The annual effective dose rates (AED) results, as illustrated in Tables 6, 7, 8, 9, 10, 11, 12, 13, 14, 15, 16, 17, 18, 19, 20, 21, 22, 23, 24, 25, and 26, followed a similar trend to that of absorbed gamma dose rates. In this regard, only MP, PA, SF, SS, and WP in Tables 15, 18, 23, 24, and 26 were 0–21, 3–4, 2–4, 0–2, and 0–3 times less than the world population-weighted average values of AED_{out} and AED_{in} rates of 0.07 and 0.41 mSv y^{-1}. Other studied industrial byproducts exhibited higher AED, both external and internal rates. The exceedance of the absorbed gamma dose and annual effective dose rates for most surveyed industrial byproducts corroborates the earlier findings: the origins, high concentrations of activity concentrations, geochemical compositions, and processes of NORs (industrial byproducts) resulted in a higher dose rate of exposure than the world average limit [17, 59].

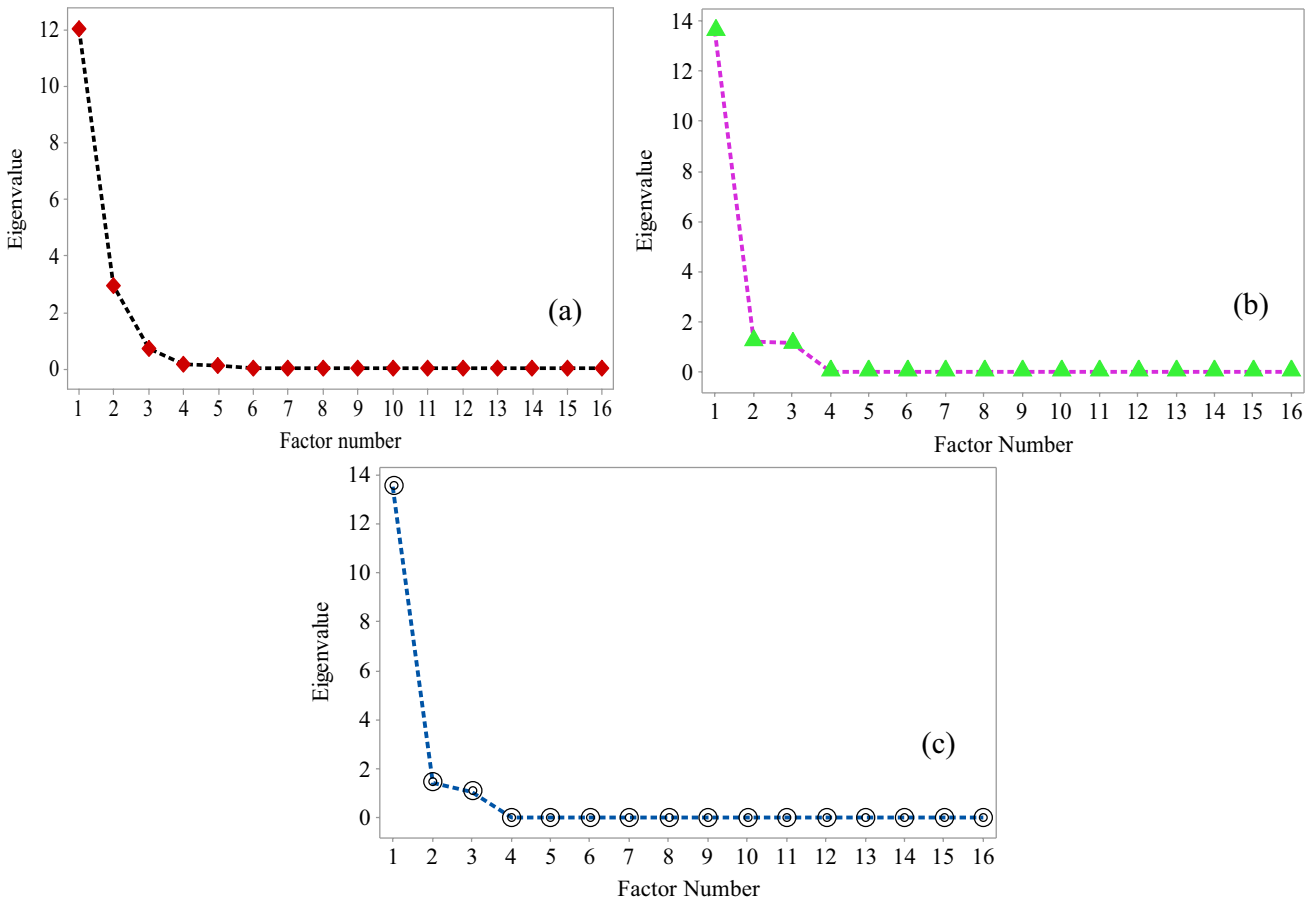

Fig. 6 The eigenvalue plots for **a** agricultural byproducts, **b** industrial byproducts (within permissible limits), and **c** industrial byproducts above permissible limits

Table 30 Rotated factor loadings of variables for agricultural and industrial byproducts

Variable	Agricultural byproducts			Industrial byproducts[&]			Industrial byproducts[*]		
	Factor 1	Factor 2	Factor 3	Factor 1	Factor 2	Factor 3	Factor 1	Factor 2	Factor 3
^{226}Ra	−0.092	−0.982	0.135	0.314	−0.949	−0.016	0.248	−0.968	−0.039
^{232}Th	0.241	−0.259	0.935	0.971	0.132	−0.201	0.979	0.083	−0.185
^{40}K	0.975	0.216	−0.042	0.075	0.017	0.997	0.122	0.053	0.991
Ra_{eq}	0.973	−0.034	0.226	0.854	−0.512	0.092	0.795	−0.570	0.210
Iγ	0.983	−0.003	0.175	0.859	−0.489	0.150	0.794	−0.533	0.292
Iα	−0.087	−0.978	0.160	0.314	−0.949	−0.016	0.248	−0.968	−0.039
H_{ex}	0.957	−0.023	0.223	0.854	−0.513	0.092	0.794	−0.570	0.209
H_{in}	0.874	−0.091	0.204	0.685	−0.726	0.053	0.617	−0.778	0.119
AUI	0.411	−0.607	0.677	0.827	−0.552	−0.110	0.764	−0.638	−0.094
AD_{out}	0.985	−0.003	0.167	0.830	−0.537	0.149	0.764	−0.580	0.283
AD_{in}	0.983	0.006	0.182	0.830	−0.537	0.149	0.764	−0.580	0.283
AED_{out}	0.986	−0.000	0.163	0.830	−0.537	0.149	0.764	−0.580	0.283
AED_{in}	0.885	−0.023	0.291	0.830	−0.537	0.149	0.764	−0.580	0.283
$ECLR_{out}$	0.985	0.004	0.170	0.830	−0.537	0.149	0.764	−0.580	0.283
$ECLR_{in}$	0.987	0.005	0.144	0.830	−0.537	0.149	0.764	−0.580	0.283
$ECLR_{total}$	0.986	0.003	0.167	0.830	−0.537	0.149	0.764	−0.580	0.283
Variability (%)	71.20	15.10	11.30	58.20	34.00	7.80	50.20	38.70	11.10

[&]Industrial byproducts within the permissible limits of world population-weighted average values

[*]Industrial byproducts above the permissible limits of world population-weighted average values

The average results of excess lifetime cancer risk, as indicated in Tables 6, 7, 8, 9, 10, 11, 12, 13, 14, 15, 16, 17, 18, 19, 20, 21, 22, 23, 24, 25, and 26, signified that all surveyed industrial byproducts, except for MP, PA, SF, SS, and WP, exceeded the UNSCEAR values of 0.29×10^{-3}, 1.16×10^{-3}, and 1.45×10^{-3} for external, internal, and total excess lifetime cancer risks. It is well known that attributing a type of cancer to radioactivity is very complex. It can only be done in cases where there are very high activity concentrations, which are not considered in this study. BA, BM, CS, FA, GGBFS, GWP, ISSA, LS, MK, MT, NS, PG, PM, RM, TS, and VA should be cautiously used to avert the risk of developing cancers when exposed to their natural radiations. Based on the established criteria, only MP, PA, SF, SS, and WP satisfied the UNSCEAR values of ^{226}Ra, ^{232}Th, ^{40}K, Ra_{eq}, I_γ, I_α, H_{ex}, H_{in}, AUI, AD, AED, and ECLR. Ultimately, MP, PA, SF, SS, and WP can safely be utilized as building and construction materials without posing any radioactive risk.

3.3 Multivariate item analysis

The Pearson correlation coefficients among all radioactive characteristics of recycled agricultural waste materials are presented in Table 27, while those of industrial byproducts are indicated in Tables 28 and 29. The larger the coefficient's absolute value, the stronger the relationship between the variables. A zero value signifies the absence of a relationship, while an absolute value of 1 represents a perfect linear correlation. Besides, a positive coefficient tends to increase or decrease together; a negative coefficient tends to increase as the other decreases. Table 27 revealed a strong linear correlation between the ^{40}K isotope and other hazard indexes. This aligns with pertinent research [118], which reported a correlation between ^{40}K and AD (0.537). The ^{40}K yielded a poor negative correlation coefficient with alpha index (I_α) (Table 28) due to a positive correlation between ^{226}Ra and I_α. As shown in Tables 28 and 29, the Pearson correlation factors for industrial byproducts indicated a strong linear correlation between the activity concentrations (^{226}Ra and ^{232}Th) and other hazard parameters. This corroborates the previous studies where the correlation between the activity concentrations (^{226}Ra and ^{232}Th) and Ra_{eq}, AD, AED, I_γ, I_α, H_{ex}, H_{in}, and AUI) of building materials yielded a good relationship [119, 120]. Furthermore, a multivariate statistical analysis of radiation risks and naturally occurring radioactive materials in lakes surrounding a petroleum industrial area in China revealed a strong positive association between some radiation risk indicators. There was no significant correlation between ^{226}Ra and ELCR or H_{ex}. However, there was a strong positive correlation between the radiation risk index and ^{232}Th, ^{226}Ra, and ^{40}K [121].

Tables 27, 28, 29 show that ^{226}Ra and ^{232}Th radionuclides generate a positive correlation but poor and negative correlation coefficients with ^{40}K. Unlike the ^{226}Ra and ^{232}Th decay series, which occur together in nature, the ^{40}K

isotope originates from a different series, exhibiting a positive correlation coefficient but yielding a poor correlation with ^{40}K [119, 120]. For various construction materials, a related study reported a good positive correlation between ^{226}Ra and ^{40}K (0.56) and a strong positive relationship between ^{232}Th and ^{40}K (0.72) [18]. These correlations may be ascribed to the mineralogical compositions of materials influencing radionuclide mobility [119]. A pertinent study also noted that the parent bodies exhibit distinct chemical behaviors in water due to the nuclides' varying decay sequence of origin. Every sampling site has a different contribution from each isotope to the overall radioactivity [121]. As shown in Table 28, a negatively poor correlation was noticed between ^{226}Ra and other hazard indexes, except with ^{232}Th, which yielded a positive relationship. A weak positive correlation was observed between ^{232}Th and other hazard indexes, except the activity utilization index (AUI), which caused a strong correlation.

The Cronbach's alpha (α) values of the radiological variables were 0.9657, 0.9842, and 0.9841 for agricultural byproducts, industrial byproducts within the permissible limits of world population-weighted average value and industrial byproducts above the allowable limits of UNSCEAR values. These signify that the radiological data are consistent and reliable. It is clear that the existence of naturally occurring radionuclides in agricultural byproducts is dependent on and greatly influenced by the presence of a ^{40}K concentration. The presence of ^{226}Ra, ^{232}Th, and ^{40}K concentrations influences the naturally occurring radionuclides in industrial byproducts.

3.4 Factor analysis

The scree (eigenvalue) plot, which provides visual information about the factors, is presented in Fig. 6a–c. Only the factors with eigenvalues greater than one are extracted and the rotated factor loadings are presented in Table 30 for the byproducts. The loading factor analysis shown in Fig. 6a–c exhibited three factors with eigenvalues greater than one. For agricultural byproducts, as summarized in Table 30, factor 1 was highly loaded with ^{40}K concentration; factor 2 was primarily loaded with ^{40}K concentration, while factor 3 was highly loaded with ^{232}Th concentration, explaining 71.20, 15.10, and 11.30% of the total variance. Industrial byproducts shown in Fig. 6b and c were loaded with ^{232}Th and ^{40}K in factors 1, 2, and 3, describing 50–59, 34–39, and 7–12% of the total variance. Factor 1 provides more underlying dimensions than factors 2 and 3. The ^{40}K isotope significantly influences the radionuclide activities of agricultural byproducts. The ^{232}Th and ^{226}Ra concentrations significantly contribute to the radionuclide activities of industrial byproducts, followed by the ^{40}K concentration. These findings are comparable to earlier research where the factor analysis revealed that radioactive hazard parameters in industrial byproducts for building materials exist due to ^{232}Th and ^{226}Ra concentration with a variance of 95.58% [36]. In addition, two primary components were identified from the available data, accounting for roughly 87.90% of the variation in radiation hazards and naturally occurring radioactive materials in the lakes surrounding a Chinese petroleum industrial area. Strong and positive relationships were found between ^{232}Th, Ra_{eq}, AED, ELCR, AD, H_{ex}, H_{in}, Annual gonadal dose equivalent (AGDE), AUI, and I_{γ}, and the first factor, accounting for 73.60% of the total variance. The second factor had substantial positive factor loadings on ^{226}Ra, ^{40}K, and electrical conductivity, accounting for 14.30% of the overall variation. Oil exploitation, agricultural production, and mestic sewage discharge may be connected to these factors [121].

4 New techniques for reducing the radiological hazards of industrial byproducts

There has been little interest in reducing the hazards associated with NORs in industrial byproducts. The reduction of radiological risks of industrial byproducts using various additives has been investigated. A pertinent study [122] established a decrease in radon release or protection of gamma radiation as driving techniques in a study that set out to reduce the effective dose due to the radioactive risks of building materials. Their research blended lightweight clay (LWC) with a 50 wt. % of fly ash (FA) for the production of LWC-FA brick. The results revealed protection from gamma radiation, which almost has the same shielding as concrete. A serious drawback of this method is that the radioactive concentrations of the used FA were unknown. Another weakness of this approach is that it failed to highlight how the shielding effect was attained.

Relevant research examined the reduction of fly ash radiation by adding 5–30 wt. % of snow into FA. Before compaction, 10% of natural snow was added to FA content [123]. The water content was fixed at 19.95% optimum, while extra water was provided via additional snow for hydration, increasing the total water content by 48% with snow melting. The FA-snow compacted samples revealed a reduction in activity concentrations of ^{235}U, ^{226}Ra, ^{232}U, and ^{232}Th by 42, 38, 31, and 31% compared with the samples without snow compaction. The reasons for this radioactive

reduction can be linked to the extra cementitious phases of calcium-silicate-hydrate and calcium-aluminate-silicate-hydrate, increasing the void ratio by 30% [123].

Phosphogypsum (PG) was addressed in producing super-sulfated cement-based concrete. Its utilization is limited due to its high radioactive emissions [2]. In this regard, Kovler et al. [124] suggested purifying PG to eliminate ^{226}Ra and heavy metals. Gijbels et al. [125] recommended using alkaline cement to immobilize the radon in PG.

A cogent research examined the various functional additives such as gypsum, barite, high alumina cement, zeolite, and ferric oxide in the radioactive reduction of fly ash-based building materials [126]. The most striking result to emerge from this investigation is the large-scale use of these additives in producing fly ash-based building materials. A blend of fly ash, cement, and sand was prepared using a replacement of 55, 20, and 25 wt. %. After that, sand was replaced with these functional additives to reduce radon and gamma emissions. The results revealed a decrease in radon and gamma release by approximately 65 and 45%. Related research [126] claimed that three mechanisms enhanced the radon protection and reduced the gamma release with these functional additives: First, the use of fine zeolite enhances the absorption of water molecules and interacts with radon, forming crystals and immobilizing them into a zeolite structure. Second, the inclusion of these additives constitutes hydrate layers on the surface of FA, increasing the phase content of calcium-silicate-hydrate and reducing the radon and gamma emissions. Third, the barium element interacts with radon and gamma-ray from ^{226}Ra, ^{232}Th, and ^{40}K, which causes photoelectron, Compton, and electron mechanisms, absorbing energy or altering the movement of gamma rays. Zeolite improved the air quality within the building by removing radioactive pollutants such as radon and organic odour-causing compounds, total volatile organic, carbon dioxide, nitrogen dioxide, carbon monoxide, bacterial, and formaldehyde [127].

Another study [128] introduced about 5–15 wt. % of silica fume into a Portland cement concrete mix. These resulted in about 3–4 and 2–3 mBq m^2 s^{-1} radon exhalation reduction rates at 7 and 28 days of curing compared with normal concrete with approximately 6 and 4 mBq m^2 s^{-1} of radon exhalation rates at days 7 and 28 days of curing. This aligns with the claims that once the quantity of additive (silica fume) is adequate to shield the particles of coarse aggregates, extra silica fume serves no purpose in setting the paste of aggregate-cement interphase [126, 129]. Mas et al. [61] found that a blend of 80 wt. % gypsum and 20 wt. % GGBFS led to lesser activity concentrations and radon equivalent activity.

Boushssa et al. [38] studied the efficiency of acid mixtures for mitigating the radioactive contaminants in phosphogypsum (PG). Phosphate rock (PR) was dehydrated at 100 °C for 24 h, ground, and sieved at ambient temperature through a 250 mm mesh aperture, producing a fine uniform powder (PG). The decompositions of PG with 65% sulfuric acid (H_2SO_4), 37% hydrochloric acid (HCl) + 65% nitric acid (HNO_3), and 37% HCl + 65% H_2SO_4 reduced the ^{226}Ra concentration to 831 ± 87, 465 ± 40, and 424 ± 32 Bq kg^{-1}, and ^{232}Th concentration to 10 ± 2, 8 ± 1, 7.83 ± 1 Bq kg^{-1} compared to PR, which exhibited 1289 ± 73 Bq kg^{-1} for ^{226}Ra and 13 ± 2 Bq kg^{-1} for ^{232}Th. The radiation hazard indexes, such as Ra_{eq}, H_{ex}, H_{in}, AD_{in}, AD_{out}, AED_{in}, and AED_{out}, decreased with the digestion of PR with sulfuric acid and either nitric or hydrochloric acid. Thus, the main cause of radium precipitation in PG, radium sulfate ($RaSO_4$), can be decreased by adding nitrogen or chlorine during the sulfuric acid digestion of phosphate rocks. This decrease is explained by the complexation of nitric or chloride with Ra, which stops radium sulfate from precipitating [38].

Overall, the insights gained from these techniques could assist in advancing methods of reducing the radiological risks of building materials incorporating recycled waste materials, leading to enhanced environmental responsibility and adherence to regulations in the use of agro-industrial byproducts.

5 Conclusions and recommendations

This study reviewed the ^{226}Ra, ^{232}Th, and ^{40}K of agro-industrial byproducts. Other radioactive index parameters were evaluated based on these activity concentrations and compared with the UNSCEAR recommendations. The study engaged the statistical analysis and reduction techniques of radioactive hazards to establish the correlations among the radiological variables and reduce the radioactive emissions. The following conclusions are drawn based on the findings:

Except for ^{40}K for RHA, POC, and POFA, which were approximately 17, 29, and 6% greater than the UNSCEAR's requirement, the activity concentrations of all reviewed recycled agricultural waste materials met the suggested mean values of UNSCEAR. Besides, their evaluated radioactive parameters satisfied the UNSCEAR's mean values. There is no possible radioactive risk when using any analyzed recycled agricultural waste products for building and construction purposes.

Only MP, PA, SF, SS, and WP (industrial byproducts) met the set criteria for the UNSCEAR's mean values of the activity concentrations, including indexes derived from them. Most of the radioactive parameters for BA, BM, CS, FA, GGBFS, GWP, ISSA, LS, MK, MT, NS, PG, PM, RM, TS, and VA (industrial byproducts) were greater than the UNSCEAR's mean values due

to exceptionally high values in some of their activity concentrations. Extreme cautions are needed in applying BA, BM, CS, FA, GGBFS, GWP, ISSA, LS, MK, MT, NS, PG, PM, RM, TS, and VA as building and construction materials.

The multivariate item approach results for distributing radioactive contents in the analyzed recycled agro-industrial materials indicate that the ^{40}K, ^{232}Th, and ^{226}Ra are mostly responsible for the radiological characteristics. The ^{40}K has a substantial impact on the radionuclide activities of agricultural byproducts, with 71.20% variability. This is followed by ^{232}Th and ^{226}Ra concentrations with 15.10% and 11.30% variability. The radioactive concentrations of industrial byproducts are mostly influenced by ^{232}Th concentration with a predominant variability of 58.20%, followed by ^{226}Ra and ^{40}K.

The methods for lowering the radiological risks posed by industrial wastes are still emerging. Adding silica fume, zeolite, lightweight clay, snow, barite, gypsum, and sulfuric, hydrochloric, and nitric acids at the required percentage replacement of recycled industrial waste materials reduces the radioactive hazards.

This research contributes to the existing knowledge of radiological characteristics of agricultural and industrial byproducts by providing a database on the potential and practical use with little or no risk. More focus should be placed on the industrial byproducts since all indicators of natural radioactivity and radioactive hazards of most industrial byproducts were exceeded. It is part of national guidelines and policies to use agro-industrial waste ash as SCMs for cement substitution. This should be based on the principle of not endangering human health. The producers of agro-industrial byproducts can regularly send samples for radiation checks to help with the production process. People should be aware of the health concerns posed by radioactivity, particularly with regard to industrial byproducts, and should be concerned if the level of radioactivity exceeds established national standards. These research findings guide the application of recycled agro-industrial wastes in the building and construction industry to lessen the harm to the public brought on by the use of radioactive elements, ensuring a safer living environment. Despite this, further studies are needed to reduce the radionuclide concentrations of industrial byproducts above the permissible limits proposed by UNSCEAR.

Author contributions S.O. conceptualized and designed the study, collected the data, analyzed and interpreted the results, analyzed the data with software, and wrote and reviewed the manuscript.

Funding The author declares that no funds, grants, or other support were received during the preparation of this manuscript.

Data availability The datasets generated during and/or analysed during the current study are available from the corresponding author on reasonable request.

Declarations

Ethics approval and consent to participate Not applicable.

Consent for publication Not applicable.

Competing interests The authors declare no competing interests.

References

1. Belaïd F. How does concrete and cement industry transformation contribute to mitigating climate change challenges? Resour Conserv Recycl Adv. 2022;15:200084. https://doi.org/10.1016/j.rcradv.2022.200084.
2. Puertas F, Suárez-Navarro JA, Alonso MM, Gascó C. NORM waste, cements, and concretes. A review. Materiales de Construcción. 2021;71:e259. https://doi.org/10.3989/mc.2021.13520.
3. Vignesh KS, Rajadesingu S, Arunachalam KD. Challenges, issues, and problems with zero-waste tools. In: Hussain CM, editor. Concepts of advanced zero waste tools. Amsterdam: Elsevier; 2021. p. 69–90.

4. Fernando Y, Tseng M-L, Sroufe R, Abideen AZ, Shaharudin MS, Jose R. Eco-innovation impacts on recycled product performance and competitiveness: Malaysian automotive industry. Sustain Prod Consum. 2021;28:1677–86. https://doi.org/10.1016/j.spc.2021.09.010.
5. Oyebisi S, Owamah H, Ede A. Flexural optimization of slag-based geopolymer concrete beams modified with corn cob ash. Scientia Iranica. 2021. https://doi.org/10.24200/sci.2021.57211.5120.
6. Tian X, Xie J, Xu M, Wang Y, Liu Y. An infinite life cycle assessment model to re-evaluate resource efficiency and environmental impacts of circular economy systems. Waste Manage. 2022;145:72–82. https://doi.org/10.1016/j.wasman.2022.04.035.
7. Council of European Union. Council Directive 2013/59/Euratom of 5 December 2013 laying down basic safety standards for protection against the dangers arising from exposure to ionizing radiation, and repealing directives 89/618/Euratom, 90/641/Euratom, 96/29/Euratom, 97/43/Euratom and 2003/122/Euratom. Off. J. Eur. United Nation. vol. 13. 2014.
8. Oyebisi S, Alomayri T. Cement-based concrete modified with Vitellaria Paradoxa ash: a lifecycle assessment. Constr Build Mater. 2022. https://doi.org/10.1016/j.conbuildmat.2022.127906.
9. Ignjatović I, Sas Z, Dragaš J, Somlai J, Kovács T. Radiological and material characterization of high volume fly ash concrete. J Environ Radioact. 2017;168:38–45. https://doi.org/10.1016/j.jenvrad.2016.06.021.
10. Khandaker MU, Jojo PJ, Kassim HA, Amin YM. Radiometric analysis of construction materials using HPGe gamma-ray spectrometry. Radiat Prot Dosim. 2012;152:33–7. https://doi.org/10.1093/rpd/ncs145.
11. European Commission. Radiological protection principles concerning the natural radioactivity of building materials, Radiation Protection Report -RP-112. Luxembourg; 1999.
12. International Atomic Energy Agency. Radiation Protection and Safety of Radiation Sources: International Basic Safety Standards. Vienna; 2014.
13. United Nations Scientific Committee on the Effects of Atomic Radiation. Sources, Effects and Risks of Ionizing Radiation. Report to the General Assembly, Scientific Annexes A, B, C and D. New York, NY; 2017.
14. Kovler K. Radioactive materials. In: Pacheco-Torgal F, Jalali S, Fucic A, editors. Toxicity of building materials. Amsterdam: Elsevier; 2012. p. 196–240.
15. Joel ES, Maxwell O, Adewoyin OO, Olawole OC, Arijaje TE, Embong Z, et al. Investigation of natural environmental radioactivity concentration in soil of coastaline area of Ado-Odo/Ota Nigeria and its radiological implications. Sci Rep. 2019;9:4219. https://doi.org/10.1038/s41598-019-40884-0.
16. United Nations Scientific Committee on the Effects of Atomic Radiation. Sources and Effects of Ionizing Radiation, United Nations Scientific Committee on the Effects of Atomic Radiation UNSCEAR 2000 Report to the General Assembly, with Scientific Annexes. New York, NY; 1993.
17. Trevisi R, Leonardi F, Risica S, Nuccetelli C. Updated database on natural radioactivity in building materials in Europe. J Environ Radioact. 2018;187:90–105. https://doi.org/10.1016/j.jenvrad.2018.01.024.
18. Legasu ML, Chaubey AK. Determination of dose derived from building materials and radiological health related effects from the indoor environment of Dessie city, Wollo. Ethiopia Heliyon. 2022;8:e09066. https://doi.org/10.1016/j.heliyon.2022.e09066.
19. Sas Z, Sha W, Soutsos M, Doherty R, Bondar D, Gijbels K, et al. Radiological characterisation of alkali-activated construction materials containing red mud, fly ash and ground granulated blast-furnace slag. Sci Total Environ. 2019;659:1496–504. https://doi.org/10.1016/j.scitotenv.2019.01.006.
20. Al-Sewaidan HA. Natural radioactivity measurements and dose rate assessment of selected ceramic and cement types used in Riyadh, Saudi Arabia. J King Saud Univ Sci. 2019;31:987–92. https://doi.org/10.1016/j.jksus.2019.04.001.
21. Vasilyev A, Yarmoshenko I, Zhukovsky M. Radon safety in terms of energy efficiency classification of buildings. IOP Conf Ser Earth Environ Sci. 2017;72:012020. https://doi.org/10.1088/1755-1315/72/1/012020.
22. United Nations Scientific Committee on the Effects of Atomic Radiation. Sources and Effects of Ionizing Radiation, United Nations Scientific Committee on the Effects of Atomic Radiation UNSCEAR 2000 Report to the General Assembly, with Scientific Annexes. New York, NY; 2000.
23. Canadian Nuclear Safety Commission. Introduction to Radiation. 2012.
24. Aladeniyi K, Arogunjo AM, Pereira AJSC, Khandaker MU, Bradley DA, Sulieman A. Evaluation of radiometric standards of major building materials used in dwellings of South-Western Nigeria. Radiat Phys Chem. 2021;178:109021. https://doi.org/10.1016/j.radphyschem.2020.109021.
25. Kocsis E, Tóth-Bodrogi E, Peka A, Adelikhah M, Kovács T. Radiological impact assessment of different building material additives. J Radioanal Nucl Chem. 2021;330:1517–26. https://doi.org/10.1007/s10967-021-07897-4.
26. World Health Organization. WHO handbook on indoor radon. Geneva: World Health Organization; 2009.
27. Darby S, Hill D, Auvinen A, Barros-Dios JM, Baysson H, Bochicchio F, et al. Radon in homes and risk of lung cancer: collaborative analysis of individual data from 13 European case-control studies. BMJ. 2005;330:223. https://doi.org/10.1136/bmj.38308.477650.63.
28. Oyebisi S, Shammas MI, Ayeni O, Samaila H. Radioactive assessments of concrete modified with recycled waste materials. Earth Sci Inform. 2025;18:126. https://doi.org/10.1007/s12145-024-01632-9.
29. Turhan Ş, Jamasali Y. Evaluation of radiological health risk caused by the use of fly ash in cement and concrete production and its storage. Int J Environ Health Res. 2024. https://doi.org/10.1080/09603123.2023.2301051.
30. Bulut HA, Şahin R. Radiological characteristics of self-compacting concretes incorporating fly ash, silica fume, and slag. J Build Eng. 2022;58:104987. https://doi.org/10.1016/j.jobe.2022.104987.
31. Alperen Bulut H, Şahin R. Activity concentration and annual effective dose assessments of radon in SCCs with different mineral additives. Constr Build Mater. 2023;364:130004. https://doi.org/10.1016/j.conbuildmat.2022.130004.
32. Sanjuán MÁ, Suárez-Navarro JA, Argiz C, Barragán M, Hernáiz G, Cortecero M, et al. Radiological characteristics of carbonated portland cement mortars made with GGBFS. Materials. 2022;15:3395. https://doi.org/10.3390/ma15093395.
33. Beretka J, Mathew PJ. Natural radioactivity of Australian building materials, Industrial Wastes and By-products. Health Phys. 1985;48:87–95. https://doi.org/10.1097/00004032-198501000-00007.

34. Rahman SU, Rafique M, Jabbar A, Matiullah. Radiological hazards due to naturally occurring radionuclides in the selected building materials used for the construction of dwellings in four districts of the Punjab Province, Pakistan. Radiat Prot Dosim. 2013;153:352–60. https://doi.org/10.1093/rpd/ncs109.
35. Li K, Zhu L, Wu Z, Wang X. Properties of cemented filling materials prepared from phosphogypsum-steel slag–blast-furnace slag and its environmental effect. Materials. 2024;17:3618. https://doi.org/10.3390/ma17143618.
36. Imani M, Adelikhah M, Shahrokhi A, Azimpour G, Yadollahi A, Kocsis E, et al. Natural radioactivity and radiological risks of common building materials used in Semnan Province dwellings, Iran. Environ Sci Pollut Res. 2021;28:41492–503. https://doi.org/10.1007/s11356-021-13469-6.
37. Pradhoshini KP, Santhanabharathi B, Chandrasekaran A, Ahmed MS, Priyadharshini M, Duong VH, et al. Radiation doses received by humans in their dwellings – a baseline report on radionuclides exposure from construction materials used in Chennai, Tamil Nadu, India. J Hazard Mater. 2025;484:136754. https://doi.org/10.1016/j.jhazmat.2024.136754.
38. Bouhssa ML, Hakkar M, Arhouni FE, Ouakkas S, Boukhair A. Efficiency of acid mixtures for mitigating the radioactive contaminants in phosphogypsum. Radiat Phys Chem. 2024;225:112152. https://doi.org/10.1016/j.radphyschem.2024.112152.
39. NORDIC. Naturally Occurring Radioactivity in the Nordic Countries – Recommendations. Denmark, Finland, Iceland, Norway and Sweden; 2000.
40. International Commission on Radiological Protection. Protection against Rn-222 at Home and at Work. ICRP Publication 65. Annals of the ICRP 3. 1994;1–48.
41. Ravisankar R, Vanasundari K, Chandrasekaran A, Rajalakshmi A, Suganya M, Vijayagopal P, et al. Measurement of natural radioactivity in building materials of Namakkal, Tamil Nadu, India using gamma-ray spectrometry. Appl Radiat Isot. 2012;70:699–704. https://doi.org/10.1016/j.apradiso.2011.12.001.
42. Caridi F, Di Bella M, Sabatino G, Belmusto G, Fede MR, Romano D, et al. Assessment of natural radioactivity and radiological risks in river sediments from Calabria (Southern Italy). Appl Sci. 2021;11:1729. https://doi.org/10.3390/app11041729.
43. Nuccetelli C, Risica S, D'Alessandro M, Trevisi R. Natural radioactivity in building material in the European Union: robustness of the activity concentration index I and comparison with a room model. J Radiol Prot. 2012;32:349–58. https://doi.org/10.1088/0952-4746/32/3/349.
44. Kolo MT, Khandaker MU, Shuaibu HK. Natural radioactivity in soils around mega coal-fired cement factory in Nigeria and its implications on human health and environment. Arab J Geosci. 2019;12:481. https://doi.org/10.1007/s12517-019-4607-6.
45. Khatun MA, Ferdous J, Haque MM. Natural radioactivity measurement and assessment of radiological hazards in some building materials used in Bangladesh. J Environ Prot (Irvine, Calif). 2018;09:1034–48. https://doi.org/10.4236/jep.2018.910064.
46. United Nations Scientific Committee on the Effects of Atomic Radiation. Effects of Ionizing Radiation: Report to the General Assembly, with Scientific Annexes,. New York, NY; 2008.
47. International Commission on Radiological Protection. Recommendations of the International Commission on Radiological Protection. Publication 60, 21(1–3). 1990.
48. Ley C, Bordas SPA. What makes data science different? A discussion involving Statistics2.0 and computational sciences. Int J Data Sci Anal. 2018;6:167–75. https://doi.org/10.1007/s41060-017-0090-x.
49. Brown T. Confirmatory factor analysis for applied research. NewYork: Guilford Press; 2015.
50. Gliner JA, Morgan GA. Research methods in applied settings: an integrated approach to design and analysis. Mahwah: Lawrence Erlbaum Associates Publishers; 2000.
51. Karim MR, Khandaker MU, Asaduzzaman Kh, Razak HA, Yusoff SB. Radiological risks assessment of building materials ingredients: palm oil clinker and fuel ash. Indoor Built Environ. 2019;28:479–91. https://doi.org/10.1177/1420326X18776705.
52. Rog L. Natural Radioactivity of Hard Coals and Coal Density Fractions of Differentiated Petrografical and Chemical Construction. Prace Naukowe GIG. Polish: Gornictwo i Srodowisko/Głowny Instytut Gornictwa; 2005.
53. Nuclear Energy Agency-Organization for Economic Co-operation and Development (NEA-OECD). Exposure to radiation from radioactivity in building materials. 1979.
54. Sas Z, Doherty R, Kovacs T, Soutsos M, Sha W, Schroeyers W. Radiological evaluation of by-products used in construction and alternative applications; part I. Preparation of a natural radioactivity database. Constr Build Mater. 2017;150:227–37. https://doi.org/10.1016/j.conbuildmat.2017.05.167.
55. Sakoda A, Ishimori Y, Yamaoka K. A comprehensive review of radon emanation measurements for mineral, rock, soil, mill tailing and fly ash. Appl Radiat Isot. 2011;69:1422–35. https://doi.org/10.1016/j.apradiso.2011.06.009.
56. Alam MN, Chowdhury MI, Kamal M, Ghose S, Matin AKMA, Ferdousi GSM. Radionuclide concentrations in mussels collected from the southern coast of Bangladesh. J Environ Radioact. 2000;47:201–12. https://doi.org/10.1016/S0265-931X(99)00038-7.
57. Krmpotić M, Rožmarić M, Barišić D. Mussels (Mytilus galloprovincialis) as a bio-indicator species in radioactivity monitoring of Eastern Adriatic coastal waters. J Environ Radioact. 2015;144:47–51. https://doi.org/10.1016/j.jenvrad.2015.02.027.
58. Walencik-Łata A, Smołka-Danielowska D. 234U, 238U, 226Ra, 228Ra and 40K concentrations in feed coal and its combustion products during technological processes in the Upper Silesian Industrial Region, Poland. Environ Pollut. 2020;267:115462. https://doi.org/10.1016/j.envpol.2020.115462.
59. Fidanchevski E, Angjusheva B, Jovanov V, Murtanovski P, Vladiceska L, Aluloska NS, et al. Technical and radiological characterisation of fly ash and bottom ash from thermal power plant. J Radioanal Nucl Chem. 2021;330:685–94. https://doi.org/10.1007/s10967-021-07980-w.
60. El Arabi AM, Ahmed NK, Salahel DK. Assessment of terrestrial gamma radiation doses for some Egyptian granite samples. Radiat Prot Dosim. 2007;128:382–5. https://doi.org/10.1093/rpd/ncm367.
61. Mas JL, Ramírez JRC, Bermúdez SH, Fernández CL. Assessment of natural radioactivity levels and radiation exposure in new building materials in Spain. Radiat Prot Dosim. 2021;194:178–85. https://doi.org/10.1093/rpd/ncab089.
62. Sahoo BK, Nathwani D, Eappen KP, Ramachandran TV, Gaware JJ, Mayya YS. Estimation of radon emanation factor in Indian building materials. Radiat Meas. 2007;42:1422–5. https://doi.org/10.1016/j.radmeas.2007.04.002.
63. Petropoulos NP, Anagnostakis MJ, Simopoulos SE. Photon attenuation, natural radioactivity content and radon exhalation rate of building materials. J Environ Radioact. 2002;61:257–69. https://doi.org/10.1016/S0265-931X(01)00132-1.

64. Amin YM, Uddin Khandaker M, Shyen AKS, Mahat RH, Nor RM, Bradley DA. Radionuclide emissions from a coal-fired power plant. Appl Radiat Isot. 2013;80:109–16. https://doi.org/10.1016/j.apradiso.2013.06.014.
65. Lu X, Li LY, Wang F, Wang L, Zhang X. Radiological hazards of coal and ash samples collected from Xi'an coal-fired power plants of China. Environ Earth Sci. 2012;66:1925–32. https://doi.org/10.1007/s12665-011-1417-x.
66. Mishra UC. Environmental impact of coal industry and thermal power plants in India. J Environ Radioact. 2004;72:35–40. https://doi.org/10.1016/S0265-931X(03)00183-8.
67. Karangelos DJ, Petropoulos NP, Anagnostakis MJ, Hinis EP, Simopoulos SE. Radiological characteristics and investigation of the radioactive equilibrium in the ashes produced in lignite-fired power plants. J Environ Radioact. 2004;77:233–46. https://doi.org/10.1016/j.jenvrad.2004.03.009.
68. Yu Q. Investigation on the radioactivity concentration of coal and ash from Shanghai coal-fired power plant, China. J Radiol Med Prot. 1996;16:374–5.
69. Tso MW, Leung JKC. Radiological impact of coal ash from the power plants in Hong Kong. J Environ Radioact. 1996;30:1–14. https://doi.org/10.1016/0265-931X(95)00042-9.
70. Xinwei L, Xiaolan Z. Measurement of natural radioactivity in sand samples collected from the Baoji Weihe Sands Park. China Environ Geol. 2006;50:977–82. https://doi.org/10.1007/s00254-006-0266-5.
71. Puch K-H, Bialucha R, Keller G. Naturally occurring radioactivity in industrial by-products from coal-fired power plants, from municipal waste incineration and from the iron- and steel-industry. Amsterdam: Elsevier; 2005. p. 996–1008.
72. Zeller B. Radioaktivitätsbilanzen in Steinkohlekraftwerken, Diplomarbeit im FB Technisches Gesundheitswesen, FIZ Gießen–Friedberg. 1995.
73. Schroeyers W, Sas Z, Bator G, Trevisi R, Nuccetelli C, Leonardi F, et al. The NORM4Building database, a tool for radiological assessment when using by-products in building materials. Constr Build Mater. 2018;159:755–67. https://doi.org/10.1016/j.conbuildmat.2017.11.037.
74. Khan IU, Sun W, Lewis E. Review of low-level background radioactivity studies conducted from 2000 to date in people Republic of China. J Radiat Res Appl Sci. 2020;13:406–15. https://doi.org/10.1080/16878507.2020.1744330.
75. Sanjuán MÁ, Quintana B, Argiz C. Coal bottom ash natural radioactivity in building materials. J Radioanal Nucl Chem. 2019;319:91–9. https://doi.org/10.1007/s10967-018-6251-0.
76. Alonso MM, Suárez-Navarro JA, Pérez-Sanz R, Gascó C, de Reyes AMM, Lanzón M, et al. Data on natural radionuclide's activity concentration of cement-based materials. Data Brief. 2020;33:106488. https://doi.org/10.1016/j.dib.2020.106488.
77. Zak A, Isajenko K, Piotrowska B, Kuczbajska M, Zabek A, Szczygielski T. Natural radioactivity of wastes. Nukleonika. 2008;55:387–91.
78. Lehmann R. Strahlenbelastung durch nat€urliche radionuklide in baumaterialien, fossilen brennstoffen und Dungemitteln. Berlin: Bundesamt fur Strahlenshutz; 1996.
79. Alonso MM, Pasko A, Gascó C, Suarez JA, Kovalchuk O, Krivenko P, et al. Radioactivity and Pb and Ni immobilization in SCM-bearing alkali-activated matrices. Constr Build Mater. 2018;159:745–54. https://doi.org/10.1016/j.conbuildmat.2017.11.119.
80. Turhan Ş. Assessment of the natural radioactivity and radiological hazards in Turkish cement and its raw materials. J Environ Radioact. 2008;99:404–14. https://doi.org/10.1016/j.jenvrad.2007.11.001.
81. Kumar V, Ramachandran TV, Prasad R. Natural radioactivity of Indian building materials and by-products. Appl Radiat Isot. 1999;51:93–6. https://doi.org/10.1016/S0969-8043(98)00154-7.
82. Gökçe HS, Canbaz Öztürk B, Çam NF, Andiç-Çakır Ö. Natural radioactivity of barite concrete shields containing commonly used supplementary materials. Constr Build Mater. 2020;236:117569. https://doi.org/10.1016/j.conbuildmat.2019.117569.
83. Ademola JA, Onyema UC. Assessment of natural radionuclides in fly ash produced at orji river thermal power station, Nigeria and the associated radiological impact. Nat Sci (Irvine). 2014;06:752–9. https://doi.org/10.4236/ns.2014.610075.
84. Mahur AK, Kumar R, Sengupta D, Prasad R. Estimation of radon exhalation rate, natural radioactivity and radiation doses in fly ash samples from Durgapur thermal power plant, West Bengal, India. J Environ Radioact. 2008;99:1289–93. https://doi.org/10.1016/j.jenvrad.2008.03.010.
85. Nuccetelli C, Pontikes Y, Leonardi F, Trevisi R. New perspectives and issues arising from the introduction of (NORM) residues in building materials: a critical assessment on the radiological behaviour. Constr Build Mater. 2015;82:323–31. https://doi.org/10.1016/j.conbuildmat.2015.01.069.
86. Peppas TK, Karfopoulos KL, Karangelos DJ, Rouni PK, Anagnostakis MJ, Simopoulos SE. Radiological and instrumental neutron activation analysis determined characteristics of size-fractionated fly ash. J Hazard Mater. 2010;181:255–62. https://doi.org/10.1016/j.jhazmat.2010.05.005.
87. Gupta M, Mahur AK, Varshney R, Sonkawade RG, Verma KD, Prasad R. Measurement of natural radioactivity and radon exhalation rate in fly ash samples from a thermal power plant and estimation of radiation doses. Radiat Meas. 2013;50:160–5. https://doi.org/10.1016/j.radmeas.2012.03.015.
88. Khandaker MU, Asaduzzaman K, Bin SAF, Bradley DA, Isinkaye MO. Elevated concentrations of naturally occurring radionuclides in heavy mineral-rich beach sands of Langkawi Island, Malaysia. Mar Pollut Bull. 2018;127:654–63. https://doi.org/10.1016/j.marpolbul.2017.12.055.
89. Feng T, Lu X. Natural radioactivity, radon exhalation rate and radiation dose of fly ash used as building materials in Xiangyang, China. Indoor Built Environ. 2016;25:626–34. https://doi.org/10.1177/1420326X15573276.
90. Temuujin J, Minjigmaa A, Davaabal B, Bayarzul U, Ankhtuya A, Jadambaa TS, et al. Utilization of radioactive high-calcium Mongolian flyash for the preparation of alkali-activated geopolymers for safe use as construction materials. Ceram Int. 2014;40:16475–83. https://doi.org/10.1016/j.ceramint.2014.07.157.
91. Tuo F, Peng X, Zhou Q, Zhang J. Assessment of natural radioactivity levels and radiological hazards in building materials. Radiat Prot Dosim. 2020;188:316–21. https://doi.org/10.1093/rpd/ncz289.
92. Puertas F, Alonso MM, Torres-Carrasco M, Rivilla P, Gasco C, Yagüe L, et al. Radiological characterization of anhydrous/hydrated cements and geopolymers. Constr Build Mater. 2015;101:1105–12. https://doi.org/10.1016/j.conbuildmat.2015.10.074.

93. Sofilić T, Barišić D, Sofilić U. Monitoring of 137Cs in electric arc furnace steel making process. J Radioanal Nucl Chem. 2010;284:615–22. https://doi.org/10.1007/s10967-010-0513-9.
94. Mustonen R. Natural radioactivity in and radon exhalation from finnish building materials. Health Phys. 1984;46:1195–203. https://doi.org/10.1097/00004032-198406000-00003.
95. Gallyas M, Török I. Natural radioactivity of raw materials and products in the cement industry. Radiat Prot Dosim. 1984;7:69–71. https://doi.org/10.1093/oxfordjournals.rpd.a082965.
96. Chinchón-Payá S, Piedecausa B, Hurtado S, Sanjuán MA, Chinchón S. Radiological impact of cement, concrete and admixtures in Spain. Radiat Meas. 2011;46:734–5. https://doi.org/10.1016/j.radmeas.2011.06.020.
97. Harb S, El-Kamel AH, Abd El-Mageed AI, Abbady A, Rashed W. Concentration of U-238, U-235, Ra-226, Th-232 and K-40 for some granite samples in eastern desert of Egypt. Proc Third Environ Phys Conf Aswan, Egypt. 2008; 335.
98. Kobeissi MA, El-Samad O, Rachidi I. Health assessment of natural radioactivity and radon exhalation rate in granites used as buildingmaterials in Lebanon. Radiat Prot Dosim. 2013;153:342–51. https://doi.org/10.1093/rpd/ncs110.
99. Pavlidou S, Koroneos A, Papastefanou C, Christofides G, Stoulos S, Vavelides M. Natural radioactivity of granites used as building materials. J Environ Radioact. 2006;89:48–60. https://doi.org/10.1016/j.jenvrad.2006.03.005.
100. Krstić D, Nikezić D, Stevanović N, Vučić D. Radioactivity of some domestic and imported building materials from South Eastern Europe. Radiat Meas. 2007;42:1731–6. https://doi.org/10.1016/j.radmeas.2007.09.001.
101. Hassan NM, Ishikawa T, Hosoda M, Sorimachi A, Tokonami S, Fukushi M, et al. Assessment of the natural radioactivity using two techniques for the measurement of radionuclide concentration in building materials used in Japan. J Radioanal Nucl Chem. 2010;283:15–21. https://doi.org/10.1007/s10967-009-0050-6.
102. Todorović N, Hansman J, Mrđa D, Nikolov J, Kardos R, Krmar M. Concentrations of 226 Ra, 232 Th and 4 0 K in industrial kaolinized granite. J Environ Radioact. 2017;168:10–4. https://doi.org/10.1016/j.jenvrad.2016.07.032.
103. Adagunodo TA, George AI, Ojoawo IA, Ojesanmi K, Ravisankar R. Radioactivity and radiological hazards from a kaolin mining field in Ifonyintedo, Nigeria. MethodsX. 2018;5:362–74. https://doi.org/10.1016/j.mex.2018.04.009.
104. Turhan Ş. Radiological impacts of the usability of clay and kaolin as raw material in manufacturing of structural building materials in Turkey. J Radiol Prot. 2009;29:75–83. https://doi.org/10.1088/0952-4746/29/1/005.
105. Righi S, Bruzzi L. Natural radioactivity and radon exhalation in building materials used in Italian dwellings. J Environ Radioact. 2006;88:158–70. https://doi.org/10.1016/j.jenvrad.2006.01.009.
106. Solak S, Turhan Ş, Uğur FA, Gören E, Gezer F, Yeğingil Z, et al. Evaluation of potential exposure risks of natural radioactivity levels emitted from building materials used in Adana, Turkey. Indoor Built Environ. 2014;23:594–602. https://doi.org/10.1177/1420326X12448075.
107. Kamunda C, Mathuthu M, Madhuku M. An assessment of radiological hazards from gold mine tailings in the Province of Gauteng in South Africa. Int J Environ Res Public Health. 2016;13:138. https://doi.org/10.3390/ijerph13010138.
108. Gezer F, Turhan Ş, Uğur FA, Gören E, Kurt MZ, Ufuktepe Y. Natural radionuclide content of disposed phosphogypsum as TENORM produced from phosphorus fertilizer industry in Turkey. Ann Nucl Energy. 2012;50:33–7. https://doi.org/10.1016/j.anucene.2012.07.018.
109. Msila X, Labuschagne F, Barnard W, Billing DG. Radioactive nuclides in phosphogypsum from the lowveld region of South Africa. S Afr J Sci. 2016;112:5. https://doi.org/10.17159/sajs.2016/20150102.
110. Santos AJG, Mazzilli BP, Fávaro DIT, Silva PSC. Partitioning of radionuclides and trace elements in phosphogypsum and its source materials based on sequential extraction methods. J Environ Radioact. 2006;87:52–61. https://doi.org/10.1016/j.jenvrad.2005.10.008.
111. Trevisi R, Risica S, D'Alessandro M, Paradiso D, Nuccetelli C. Natural radioactivity in building materials in the European Union: a database and an estimate of radiological significance. J Environ Radioact. 2012;105:11–20. https://doi.org/10.1016/j.jenvrad.2011.10.001.
112. Okeji MC, Agwu KK, Idigo FU. Assessment of natural radioactivity in phosphate ore, phosphogypsum and soil samples around a phosphate fertilizer plant in Nigeria. Bull Environ Contam Toxicol. 2012;89:1078–81. https://doi.org/10.1007/s00128-012-0811-8.
113. Roper AR, Stabin MG, Delapp RC, Kosson DS. Analysis of naturally-occurring radionuclides in coal combustion fly ash, gypsum, and scrubber residue samples. Health Phys. 2013;104:264–9. https://doi.org/10.1097/HP.0b013e318279f3bf.
114. Xhixha G, Bezzon GP, Broggini C, Buso GP, Caciolli A, Callegari I, et al. The worldwide NORM production and a fully automated gamma-ray spectrometer for their characterization. J Radioanal Nucl Chem. 2013;295:445–57. https://doi.org/10.1007/s10967-012-1791-1.
115. Rubinos DA, Barral MT. Fractionation and mobility of metals in bauxite red mud. Environ Sci Pollut Res. 2013;20:7787–802. https://doi.org/10.1007/s11356-013-1477-4.
116. Somlai J, Jobbágy V, Kovács J, Tarján S, Kovács T. Radiological aspects of the usability of red mud as building material additive. J Hazard Mater. 2008;150:541–5. https://doi.org/10.1016/j.jhazmat.2007.05.004.
117. Singovszka E, Estokova A, Mitterpach J. Radioactivity of buildings materials available in Slovakia. IOP Conf Ser Earth Environ Sci. 2017;92:012054. https://doi.org/10.1088/1755-1315/92/1/012054.
118. Chandrasekaran A, Ravisankar R, Senthilkumar G, Thillaivelavan K, Dhinakaran B, Vijayagopal P, et al. Spatial distribution and lifetime cancer risk due to gamma radioactivity in Yelagiri Hills, Tamilnadu, India. Egypt J Basic Appl Sci. 2014;1:38–48. https://doi.org/10.1016/j.ejbas.2014.02.001.
119. Raghu Y, Ravisankar R, Chandrasekaran A, Vijayagopal P, Venkatraman B. Assessment of natural radioactivity and radiological hazards in building materials used in the Tiruvannamalai District, Tamilnadu, India, using a statistical approach. J Taibah Univ Sci. 2017;11:523–33. https://doi.org/10.1016/j.jtusci.2015.08.004.
120. Ravisankar R, Vanasundari K, Suganya M, Raghu Y, Rajalakshmi A, Chandrasekaran A, et al. Multivariate statistical analysis of radiological data of building materials used in Tiruvannamalai, Tamilnadu, India. Appl Radiat Isotopes. 2014;85:114–27. https://doi.org/10.1016/j.apradiso.2013.12.005.
121. Shi Y, Zhao J, Ding B, Zhang Y, Li Z, Ali MMM, et al. Multivariate statistical study on naturally occurring radioactive materials and radiation hazards in lakes around a Chinese petroleum industrial area. Nucl Eng Technol. 2024;56:2182–9. https://doi.org/10.1016/j.net.2024.01.027.
122. Mann HS, Brar GS, Mudahar GS. Gamma-ray shielding effectiveness of novel light-weight clay-flyash bricks. Radiat Phys Chem. 2016;127:97–101. https://doi.org/10.1016/j.radphyschem.2016.06.013.

123. Baykal G, Saygılı A. A new technique to reduce the radioactivity of fly ash utilized in the construction industry. Fuel. 2011;90:1612–7. https://doi.org/10.1016/j.fuel.2011.01.006.
124. Kovler K, DB, KDS, RY,. US Patent: system and methods for removing impurities from phosphogypsum and manufacturing gypsum binder. US 2017/0022070A1., 2017.
125. Gijbels K, Ion Iacobescu R, Pontikes Y, Vandevenne N, Schreurs S, Schroeyers W. Radon immobilization potential of alkali-activated materials containing ground granulated blast furnace slag and phosphogypsum. Constr Build Mater. 2018;184:68–75. https://doi.org/10.1016/j.conbuildmat.2018.06.162.
126. He D, Yin G, Dong F, Liu L, Luo Y. Research on the additives to reduce radioactive pollutants in the building materials containing fly ash. J Hazard Mater. 2010;177:573–81. https://doi.org/10.1016/j.jhazmat.2009.12.071.
127. Davies PR, RG, M-SIA, NBMC, SJFG,. Method and apparatus for improving the air quality within a building or enclosed space. 2002.
128. Yu KN, Balendran RV, Koo SY, Cheung T. Silica fume as a radon retardant from concrete. Environ Sci Technol. 2000;34:2284–7. https://doi.org/10.1021/es991134j.
129. Neville AM. Properties of concrete. 4th ed. Harlow: Longman; 2011.